NTNU
Innovation and Creativity

Geometric integration of nonlinear wave equations

Morten Lien Dahlby

Master of Science in Physics and Mathematics
Submission date: July 2007
Supervisor: Brynjulf Owren, MATH

Norwegian University of Science and Technology
Department of Mathematical Sciences

Problem Description

The thesis aim at introducing numerical schemes for nonlinear wave equations, especially the Camassa-Holm equation. One will be studying methods which possess good conservation properties, such as Lie group integrators and multisymplectic methods. The new methods should be compared to the existing methods. It will be of interest to derive the Camassa-Holm equation in a geometrical setting and also characterise its conservation laws.

Assignment given: 15. January 2007
Supervisor: Brynjulf Owren, MATH

Preface

This master's thesis was completed as part of the Master of Technology programme at the Norwegian University of Technology and Science (NTNU). It was carried out at the Department of Mathematical Sciences in the period January-July 2007.

I would like to thank my supervisor Professor Brynjulf Owren for helpful ideas, thoughts and suggestions throughout this thesis. I also wish to thank Xavier Raynaud for helping me understand how to implement some of the methods. Finally I would like to thank *the Isaac Newton Institute for Mathematical Sciences* at Cambridge University for inviting me to the programme *Highly Oscillatory Problems: Computation, Theory and Application* in June 2007. Not only did I get the chance to meet some of the giants of the trade, I also got time to go sightseeing in the beautiful town of Cambridge.

Trondheim, July 2007

Morten Dahlby

Abstract

We give an short introduction to the Camassa-Holm equation and its travelling wave solutions. Many well-known equations in mathematical physics describe geodesic flows on appropriate Lie groups. The choice of group and metric defines the Euler equation. We show that by choosing the group of diffeomorphisms on the circle and the Sobolev H^1-metric one gets the Camassa-Holm equation. The equation is shown to have a bi-Hamiltonian structure, and thus infinitely many conserved quantities.

We introduce a new class of methods that can be applied to the Euler equation. We solve the Camassa-Holm equation by freezing some of the coefficients in the Euler equation and applying a Lie group integrator. In some situations the method is found to outperform existing schemes.

The available numerical methods is reviewed and modified. We compare long term structure preservation for both smooth and non-smooth initial conditions for each method. Of special interest is the ability to handle wave collisions.

Contents

1 The Camassa-Holm equation

Geometric integration is a new branch of numerical analysis which aims to reproduce the qualitative features of the solution of the differential equation which is being discretised, in particular its geometric properties. The motivation for developing such structure-preserving algorithms arises independently in areas of research as diverse as celestial mechanics, molecular dynamics, control theory, particle accelerators physics, and numerical analysis. Although diverse, the systems appearing in these areas have one important common feature. They all preserve some underlying geometric structure which influences the qualitative nature of the phenomena they produce. In geometric integration these properties are built into the numerical method, which gives the method an improved qualitative behaviour, but also allows for a significantly more accurate long-time integration than with general-purpose methods.

In this thesis we will study the Camassa-Holm equation

$$u_t - u_{xxt} + 3uu_x - 2u_x u_{xx} - uu_{xxx} = 0 \tag{1.1}$$

and solve this equations using both conventional numerical methods and geometric integrators. The Camassa-Holm equation was first derived in 1981 [21] in a general context, however it did not get much attention. It was then rediscovered by Roberto Camassa and Darryl D. Holm in [9] and [10] a decade later. The equation can also be written as

$$\begin{aligned} m_t &= -2mu_x - m_x u \\ m &= u - u_{xx} \end{aligned} \tag{1.2}$$

A third often used formulation is

$$\begin{aligned} u_t + uu_x + P_x &= 0 \\ P - P_{xx} &= u^2 + \frac{1}{2}u_x^2 \end{aligned} \tag{1.3}$$

The Camassa-Holm equation models the unidirectional propagation of shallow water waves over a flat bottom. u represents the height of the water's free surface, t is time and x the spatial variable. m is sometimes called the momentum and P is referred to as the pressure. The equation has travelling wave solutions which is called peakons. A single peakon is given by

$$u(x,t) = ce^{-|x-ct|}, \qquad c \in \mathbb{R} \tag{1.4}$$

In the periodic case on the interval $[-\frac{a}{2}, \frac{a}{2}]$ the peakon is given by

$$u(x,t) = \frac{\cosh(\min(x, a-x))}{\sinh(\frac{a}{2})} \tag{1.5}$$

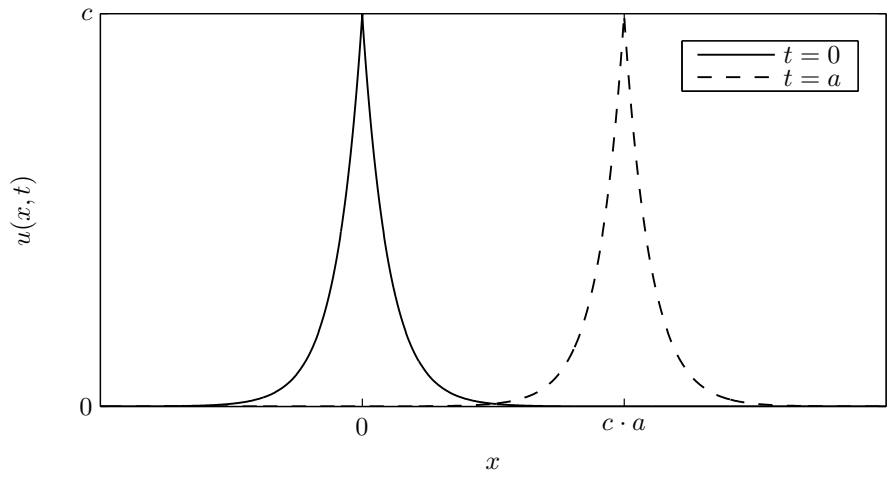

Figure 1: Peakon solution (1.4) of the Camassa-Holm equation (1.1). Notice that the travelling velocity of the wave equals its height.

The derivative is discontinuous at the peaks, therefore the peakon can only be a solution of (1.1) in a weak sense. See [22] and [35] for the conditions for local existence and well-posedness. The CH equation is in general not well posed; the first derivative of a solution can become infinite in finite time. For proofs of global existence of solutions, see [19], [15] and [43].

A linear combination of peakons is called a multipeakon solution. Multipeakons are given by (see [24])

$$u(x,t) = \sum_{i=1}^{n} p_i(t) \mathrm{e}^{-|x-q_i(t)|}$$

where $(p_i(t), q_i(t))$ is the height and the position of the peakon; they satisfy the explicit system of ordinary differential equations

$$\dot{q}_i = \sum_{j=1}^{n} p_j \mathrm{e}^{-|q_i-q_j|}, \qquad \dot{p}_i = \sum_{j=1}^{n} p_i p_j \mathrm{sgn}(q_i - q_j) \mathrm{e}^{|q_i-q_j|} \tag{1.6}$$

This system of equations is Hamiltonian: for H given by

$$H = \frac{1}{2} \sum_{i,j=1}^{n} p_i p_j \mathrm{e}^{|q_i-q_j|}$$

it can be written as

$$\dot{q}_i = \frac{\partial H}{\partial p_i}, \qquad \dot{p}_i = -\frac{\partial H}{\partial q_i}$$

Since taller waves will eventually catch up with lower waves we get peakon interactions like the one in figure 2. The waves exchange mass, but

note that the peaks remain distinct. An interesting problem arises when two equal but opposite peakons collide, this is called a peakon-antipeakon collision. At the collision ($t = 0$) both peakons vanish, but it is not exactly clear what happens for $t > 0$. Two possibilities are illustrated in the figures 3 and 4.

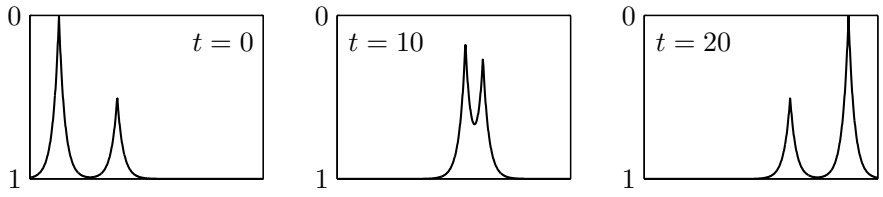

Figure 2: Peakon interactions. Apart from a phase shift, both the peakons re-emerge unaffected by the collison.

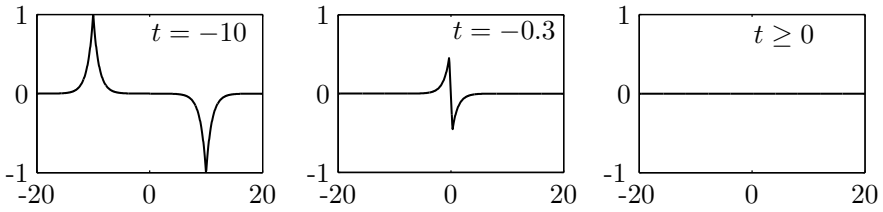

Figure 3: This scenario is called the dissipative solution since it gradually disappears. By inserting $u = 0$ into (1.1) we easily see that this is a possible solution.

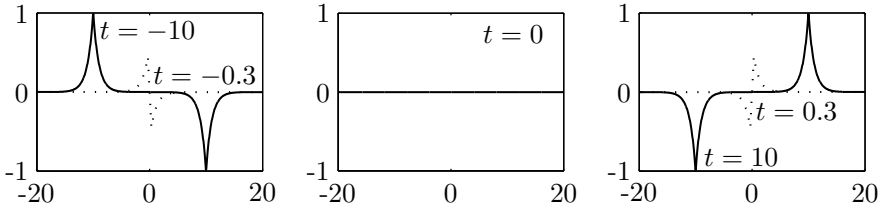

Figure 4: The second scenario is called the conservative solution since the energy is conserved. Note that both peakons re-emerge after the collision. See [5] and [6] for more information about multipeakons.

In addition to travelling wave interactions the CH equation also models wave breaking, see [16]. Wave breaking occurs when the profile of u steepens gradually and ultimately the slope becomes vertical. This is an important physical phenomenon not captured by other shallow water models, as for example the KdV equation.

It can also be shown that the CH equation has a smooth travelling wave solution [29, 28]. This can be done by inserting $u(x,t) = f(x-ct)$ into (1.1) which yields the differential equation

$$\frac{\mathrm{d}^2 f}{\mathrm{d}x^2} = f - \frac{\alpha}{(f-c)^2} \tag{1.7}$$

where c is the velocity of the wave and α is some integration constant. We consider the solution on the interval $[0, a]$, to solve this equation one needs initial conditions for both $f(x)$ and $f'(x)$. Since we want our periodic solution to be as smooth as possible, we set $f'(0) = 0 = f'(a)$ and thus making sure that the solution has a continious first derivative. By choosing c, α and $f(0)$ and integrating the solution numerically until $f(0) = f(a)$ we can get infinitely many different smooth periodic travelling waves. See figure 5 for some examples.

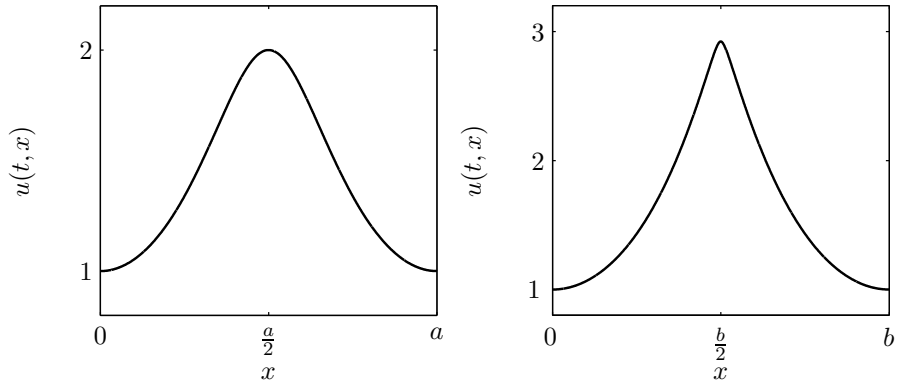

Figure 5: The solution of (1.7) with $c = 3$ and $f(0) = 1$. α is 3 on the left and 0.3 on the right which gives the periods $a \approx 6.5$ and $b \approx 3.7$ respectively. The wave gets closer to a peakon as α decreases, while a larger α will stretch the wave out.

For a more thorough review of the CH equation see the introduction of Xavier Raynaud's doctoral thesis and the references therein.

In chapter 1.1 we derive the Camassa-Holm equation as a geodesic flow on an appropriate group. This is the geometrical approach introduced by Arnold and Khesin and gives a general procedure for deriving many well-known equations in mathematical physics. Chapter 1.2 considers the theory required to prove that the Camassa-Holm equation has a bi-Hamiltonian structure, and thus infinitely many conservation laws.

In chapter 2 we review some numerical methods applied to the Camassa-Holm equation. These include finite difference methods 2.1, spectral methods 2.2, multisymplectic methods 2.3, a new class of methods based on the Euler equation 2.4 and multipeakon methods 2.5. Numerical tests are performed to better understand how the methods behave.

Finally Chapter 3 does a more thorough comparison of the numerical methods. The tests will show how the methods conserve the Hamiltonians found in chapter 1.2, how the global error behaves in the short and long term and also the running time.

1.1 Derivation

Camassa and Holm [9] proved their equation (1.1) from a physical point of view, we will arrive at the same equation using a geometrical approach initiated by Arnold in [2, 1] and the book by Arnold and Khesin [3]. Constantin and Kolev used a similar procedure in [17] and [18].

Theorem 1.1. *The Euler equation describing the geodesic flow on the Lie group of diffeomorphisms on the circle $\mathcal{D}(S^1)$ with respect to the right-invariant Sobolev H^1-metric is the Camassa-Holm equation* (1.1).

Before we are ready to prove this theorem we need some definitions to clarify what it states. We will also need to delve into Lie group theory, although I will try to be brief and only include what is necessary to prove the main theorem. For more information about Lie groups and Lie algebras see the books [40, 42].

A Lie group G is a group which is also a real smooth manifold, and in which the group operations of multiplication and inversion are smooth maps. Since a Lie group is a smooth manifold it makes sense to talk about the tangent space to that manifold, and in particular the tangent space at the identity of the group, T_eG. That tangent space is called a Lie algebra $\mathfrak{g}$. $\mathfrak{g}$ is a vector space together with a binary operation $[\cdot,\cdot] : \mathfrak{g} \times \mathfrak{g} \mapsto \mathfrak{g}$ called the Lie bracket. The Lie bracket is bilinear, skew-symmetric and satisfies the Jacobi identity

$$[u,[v,w]] + [w,[u,v]] + [v,[w,u]] = 0, \qquad \forall u,v,w \in \mathfrak{g} \tag{1.8}$$

An example of a Lie group is the group of volume preserving diffeomorphisms on the domain M, sometimes denoted $Diff(M)$ or $\mathcal{D}(M)$. A diffeomorphism is an invertible function that maps one differentiable manifold to another, such that both the function and its inverse are smooth. $\mathcal{D}(M)$ can be regarded as the configuration space ("all possible permutations of particles") of an incompressible fluid filling the domain M. The domain mentioned in theorem 1.1 is the circle S^1, thus giving the Lie group $\mathcal{D}(S^1)$. The corresponding Lie algebra called $vect(S^1)$ or $\mathfrak{d}(S^1)$ consists of divergence free veector fields in S^1 equipped with the Lie bracket

$$[u,v] = uv_x - u_x v, \qquad \forall u,v \in \mathfrak{g} \tag{1.9}$$

Another example we might encounter is the Virasoro group Vir and the corresponding algebra vir. The Virasoro algebra is given as a central extension of vector fields on the circle: $vir = vect(S^1) \oplus \mathbb{R}$.

Right and left translations are denoted, respectively, as $R_h(g) = gh$ and $L_h(g) = hg$ for $g,h \in G$. The composition of both, $A_g = R_{g^{-1}} L_g$, is called an inner automorphism. A right-translation of $g \in \mathcal{D}(M)$, that is $R_h(g) = gh$, means that the diffeomorphism h acts first, before the diffeomorphism g

changing with the velocity $\dot{g}$. This can be regarded as a renumeration of particles, and does not change the kinetic energy. We say that the kinetic energy is invariant with respect to the right-translations on the group $\mathcal{D}(M)$.

Definition 1.1. The differential of A_g at the group unity e is called the group adjoint operator

$$\mathrm{Ad}_g : \mathfrak{g} \mapsto \mathfrak{g}, \qquad \mathrm{Ad}_g u = (A_{g*}|_e)u, \qquad u \in \mathfrak{g}$$

where $F_*|_x : T_xM \mapsto T_{F(x)}M$ denotes the derivative of the mapping $F : M \mapsto M$ at x. The adjoint representation of the Lie algebra is defined as

$$\mathrm{ad}_\xi = \frac{\mathrm{d}}{\mathrm{d}t}|_{t=0}\mathrm{Ad}_{g(t)}$$

where $g(t)$ is a curve on the group G issued from the point $g(0) = e$ with the velocity $\dot{g}(0) = \xi$.

If $G = \mathcal{D}(S^1)$ we get the useful relation

$$\mathrm{ad}_u v = [u, v], \qquad u, v \in \mathfrak{g} \tag{1.10}$$

The vector space $\mathfrak{g}^*$ is the dual to the Lie algebra $\mathfrak{g}$. Thus, $\mathfrak{g}^*$ consists of all linear functionals on $\mathfrak{g}$. To every linear operator $A : X \mapsto Y$ one can associate the adjoint operator acting in the reverse direction between the corresponding dual spaces $A^* : Y^* \mapsto X^*$. It is defined by

$$(A^* y)(x) = y(Ax)$$

for $x \in X$ and $y \in Y^*$. We will be going back and forth between the Lie algebra $\mathfrak{g}$ and its dual $\mathfrak{g}^*$, the next definition tells us how.

Definition 1.2. The coadjoint (anti)representation of a Lie group G in the space $\mathfrak{g}^*$ dual to the Lie algebra $\mathfrak{g}$ is the (anti)representation that to each group element g associates the linear transformation

$$\mathrm{Ad}^*_g : \mathfrak{g}^* \mapsto \mathfrak{g}^*$$

dual to the transformation $\mathrm{Ad}_g : \mathfrak{g} \mapsto \mathfrak{g}$. In other words

$$(\mathrm{Ad}^*_g w)(u) = w(\mathrm{Ad}_g u)$$

for every $g \in G$, $w \in \mathfrak{g}^*$ and $u \in \mathfrak{g}$. Similarly the operator of the coadjoint representation of an element $v \in \mathfrak{g}$ is denoted by

$$\mathrm{ad}^*_v : \mathfrak{g}^* \mapsto \mathfrak{g}^*$$

That is

$$\mathrm{ad}^*_v w(u) = w(\mathrm{ad}_v u) \tag{1.11}$$

for every $v, u \in \mathfrak{g}$ and $w \in \mathfrak{g}^*$.

This brief introduction to Lie algebras does not do the subject justice, however a thorough study would take too much space. We will mostly need the relations (1.10) and (1.11) in this thesis. We will also need to manipulate expressions containing inner products (also called metrics) and pairings. The connection between these two is given by the inertia operator $A : \mathfrak{g} \mapsto \mathfrak{g}^*$, which is defined as:

$$(Au, v) = \langle u, v \rangle, \qquad u, v \in \mathfrak{g}$$

where $\langle \cdot, \cdot \rangle$ is the inner product on $\mathfrak{g}$ and $(\cdot, \cdot)$ is the natural pairing of elements from $\mathfrak{g}^*$ and $\mathfrak{g}$

$$(m, v) = \int mv \, \mathrm{d}x, \qquad m \in \mathfrak{g}^*, v \in \mathfrak{g}$$

Some examples of inner products are given below

$$\begin{aligned} \langle u, v \rangle_{L^2} &= \int uv \, \mathrm{d}x \\ \langle u, v \rangle_{H^1} &= \int (uv + u_x v_x) \, \mathrm{d}x \\ \langle u, v \rangle_{\dot{H}^1} &= \int u_x v_x \, \mathrm{d}x \end{aligned}$$

The inertia operator for the H^1 inner product gives

$$(m, v) = (Au, v) = \langle u, v \rangle = \int (uv + u_x v_x) \, \mathrm{d}x = \int (uv - u_{xx} v) \, \mathrm{d}x = (u - u_{xx}, v)$$

Thus $m = u - u_{xx}$. The penultimate equality follows from partial integration. We always assume that the solution is periodic or that it vanishes at infinity such that the boundary terms vanish when doing partial integration.

The only phrase in theorem 1.1 left to explain is the Euler equation or, as it is sometimes called, the Euler-Poincaré equation. It is given as:

$$\frac{\mathrm{d}m}{\mathrm{d}t} = \mathrm{ad}^*_u m, \tag{1.12}$$

where $m = Au$ and $u \in \mathfrak{g}$. Euler found this equation in [20], proofs can also be found in [32] or section 13.8 in [37]. The equation describes the geodesic flow on G with respect to a given metric and represents the extremals of the least action principle, i.e., the actual motions of the physical system. We now turn to the proof of the main theorem 1.1.

Proof of theorem 1.1. Calculating the Euler-Poincaré equation with respect to the H^1 inner product yields, and using (1.11), (1.10), (1.9) and partial

integration yields

$$\begin{aligned}(\frac{\mathrm{d}m}{\mathrm{d}t}, v) &= (\mathrm{ad}_u^* m, v) = (m, \mathrm{ad}_u v) = (m, [u, v]) \\ &= (m, uv_x - u_x v) = \int m(uv_x - u_x v)\,\mathrm{d}x = \int (-(mu)_x - mu_x)\,\mathrm{d}x \\ &= (-3uu_x + 2uu_x + uu_{xxx}, v)\end{aligned}$$

which is the Camassa-Holm equation (1.1). □

Alternatively one can choose the L^2 inner product

$$(m, v) = \langle u, v\rangle = \int uv\,\mathrm{d}x = (u, v)$$

In this case $m = u$. The Euler-Poincaré equation (1.12) then yields the inviscid Burgers equation

$$\begin{aligned}(\frac{\mathrm{d}m}{\mathrm{d}t}, v) &= \int (-(mu)_x - mu_x)\,\mathrm{d}x = \int (u^2 v_x - uu_x v)\,\mathrm{d}x \\ &= \int (-(u^2)_x - uu_x)v\,\mathrm{d}x = (-3uu_x, v)\end{aligned}$$

By scaling the time we get the more familiar version $\frac{\mathrm{d}m}{\mathrm{d}t} + uu_x = 0$.

Let us recapitulate what we just did; we started with the Euler equation which describes the geodesic flow on a Lie group. We then chose the Lie group $G = \mathcal{D}(S^1)$, and got the Lie algebra $\mathfrak{g} = \mathfrak{d}(S^1)$ and its dual $\mathfrak{g}^* = \mathfrak{d}^*(S^1)$ into the bargain. The other choice we made was to equip the Lie algebra with the H^1 inner product which defines the inertia operator A and with that $m = Au$. Calculating the Euler equation gave us the Camassa-Holm equation.

Notice that we only made two choices: the Lie group and the inner product. It is interesting to note that many well-known equations in mathematical physics can be derived using this approach. For example the Virasoro group together with the L^2 inner product yield the Korteweg-de Vries equation

$$u_t + 6uu_x + u_{xxx} = 0$$

while the Virasoro group together with the $\dot{H}^1$ inner product give the Hunter-Saxton equation

$$u_{txx} + 2u_x u_{xx} + uu_{xxx} = 0$$

And we have already shown that $\mathcal{D}(S^1)$ together with the H^1 inner product yields the Camassa-Holm equation and $\mathcal{D}(S^1)$ together with the L^2 inner product yields the Burgers equation. See [31] for a list of more equations or [3] for more details.

1.2 A bi-Hamiltonian system

The Camassa-Holm equation (1.1) can be written in Hamiltonian form in *two* ways, we say it can be expressed as a bi-Hamiltonian system. In this chapter we will define what this means and prove that it leads to an infinite hierarchy of conservation laws. We will be following the methodology of [40].

The role of the Hamiltonian function will be played by a Hamiltonian functional $\mathscr{H} = \int H \, \mathrm{d}x$ and the gradient operation is replaced by the variational derivative. Recall that $\delta\mathscr{H}[m]$ is the variational derivative of $\mathscr{H}$ at m if

$$\left.\frac{\mathrm{d}}{\mathrm{d}\epsilon}\right|_{\epsilon=0} \mathscr{H}[m + \epsilon v] = \int \delta\mathscr{H}[m] \cdot v \, \mathrm{d}x \tag{1.13}$$

A linear operator $\mathscr{D}$ is Hamiltonian if its bi-linear Poisson bracket

$$\{\mathscr{P}, \mathscr{Q}\} = \int \delta\mathscr{P} \cdot \mathscr{D}\delta\mathscr{Q} \, \mathrm{d}x \tag{1.14}$$

is skew-symmetric and satisfies the Jacobi identity (1.8) for all functionals $\mathscr{P}$ and $\mathscr{Q}$. A pair of skew-adjoint differential operators $\mathscr{D}$ and $\mathscr{E}$ is said to be a Hamiltonian pair if every linear combination is a Hamiltonian operator. A system is said to be bi-Hamiltonian if it can be written on the form

$$\frac{\partial m}{\partial t} = K_1[m] = \mathscr{D}\delta\mathscr{H}_1 = \mathscr{E}\delta\mathscr{H}_0$$

where $\mathscr{D}$ and $\mathscr{E}$ are a Hamiltonian pair and $\mathscr{H}_0[m]$ and $\mathscr{H}_1[m]$ are appropriate Hamiltonian functionals. The following proposition gives us an easy way to check if a Poisson bracket is skew-symmetric.

Proposition 1.2. *Let $\mathscr{D}$ be a $q \times q$ matrix differential operator with bracket* (1.14) *on the space of functionals. The the bracket is skew-symmetric if and only if $\mathscr{D}$ is skew-adjoint: $\mathscr{D}^* = -\mathscr{D}$.*

Proof. The skew-symmetry condition implies

$$\begin{aligned}\int \delta\mathscr{P} \cdot \mathscr{D}\delta\mathscr{Q} \, \mathrm{d}x &= -\int \delta\mathscr{Q} \cdot \mathscr{D}\delta\mathscr{P} \, \mathrm{d}x \\ &= -\int \delta\mathscr{P} \cdot \mathscr{D}^*\delta\mathscr{Q} \, \mathrm{d}x\end{aligned}$$

Which means that

$$\int \delta\mathscr{P} \cdot (\mathscr{D} + \mathscr{D}^*)\delta\mathscr{Q} \, \mathrm{d}x = 0$$

and we must have $\mathscr{D} + \mathscr{D}^* = 0$. □

Any differential operator $\mathscr{D} = \sum_i P_i[m]D_i$ has an adjoint given by

$$\mathscr{D}^* = \sum_i (-D)_i \cdot P_i[m] \tag{1.15}$$

where the i-th total derivative of P has the general form

$$D_i P = \frac{\partial P}{\partial x^i} + \sum_{\alpha=1}^{q} \sum_J m^\alpha_{J,i} \frac{\partial P}{\partial m^\alpha_J}$$

where $m = (m^1, \ldots, m^q)$ and the multi-index notation $J = (j_1, \ldots, j_k)$, such that

$$m^\alpha_{J,i} = \frac{\partial m^\alpha_J}{\partial x^i} = \frac{\partial^{k+1} m^\alpha}{\partial x^i \partial x^{j_1} \cdots \partial x^{j_k}}$$

This gives us an easy way to determine if an operator is skew-symmetric. Unfortunately checking if an operator satisfies the Jacobi identity is a complicated task, even for the simplest operators. We wish to develop a method to easily check the Jacobi identity and thus establish whether an operator is Hamiltonian. To do this we need to embark on some definitions.

Definition 1.3. Let $Q[m] = (Q_1[m], \ldots, Q_q[m])$ be a q-tuple of differentiable functions. The evolutionary generalized vector field is given by

$$\mathbf{v} = \sum_{\alpha=1}^{q} Q_\alpha[m] \frac{\partial}{\partial m^\alpha}$$

Its prolongation is the sum

$$\text{pr } \mathbf{v}_Q = \sum_{\alpha, J} D_J Q_\alpha \frac{\partial}{\partial m^\alpha_J}$$

For $\mathscr{D} = \sum_K P_K[m]D_K$ we can write

$$\text{pr } \mathbf{v}_Q(\mathscr{D}) = \sum_K \text{pr } \mathbf{v}_Q(P_K) D_K$$

As an example, suppose that we have one independent variable x and one dependent variable $m(x)$, that is $p = 1$ and $q = 1$ respectively. Also suppose $P = P(x, m, m_x, m_{xx}, m_{xxx})$ depends only on third derivatives, then the prolongation becomes:

$$\text{pr } \mathbf{v}_Q(P) = Q\frac{\partial P}{\partial m} + D_x Q \frac{\partial P}{\partial m_x} + D_x^2 Q \frac{\partial P}{\partial m_{xx}} + D_x^3 Q \frac{\partial P}{\partial m_{xxx}}$$

Notice that if $\mathscr{D}$ does not depend on m or any of its derivatives, then $\text{pr } \mathbf{v}_Q(\mathscr{D}) = 0$ for any Q.

To apply the next theorem one needs to know some properties of *forms* and the so-called *wedge product*. Simply put, forms are linear maps from a vector space to the real line. For example a 1-form is a map $\omega^1 : \mathbb{R}^n \mapsto \mathbb{R}$, while a 2-form is a map $\omega^2 : \mathbb{R}\times\mathbb{R} \mapsto \mathbb{R}$ which is bilinear and skew-symmetric. Differential forms are forms which take vectors in a tangent space as inputs.

Definition 1.4. Let M be a smooth manifold and $TM|_x$ its tangent space at x. The space $\bigwedge_k T^* M|_x$ of differential k-forms at x is the set of all k-linear alternating functions

$$\omega : TM|_x \times \cdots \times TM|_x \mapsto \mathbb{R}$$

Given a collection of 1-forms $\omega_1, \ldots, \omega_k$, we can form a differential k-form $\omega_1 \wedge \cdots \wedge \omega_2$ called the wedge product. The wedge product is multi-linear and alternating. Specifically, assume that ω, θ, ζ are 1-forms in a vector space V, then the wedge product has the following properties

$$\begin{aligned} \omega \wedge \theta &= -\theta \wedge \omega, && \text{skew-symmetric} \\ (\omega \wedge \theta) \wedge \zeta &= \omega \wedge (\theta \wedge \zeta), && \text{associative} \\ (a\omega + b\theta) \wedge \zeta &= a(\omega \wedge \zeta) + b(\theta \wedge \zeta) \\ \omega \wedge (a\theta + b\zeta) &= a(\omega \wedge \theta) + b(\omega \wedge \zeta) && \text{bilinear} \end{aligned}$$

Note that the first property implies $\omega \wedge \omega = 0$ for all $\omega \in V$. Obviously, this is a gross simplification of the extensive theory of k-forms and the wedge product. Much of the theory is omitted because it is not relevant to our usage in this thesis. The following theorem will form the tool for determing if a system is bi-Hamiltonian. The proof of this theorem is fairly elaborate and rather than just copy the results, we refer the interested reader to chapter 7 of Olver's book [40].

Theorem 1.3. *1. Let $\mathscr{D}$ be a skew-adjoint differential operator and $\Theta_{\mathscr{D}} = \frac{1}{2}\int \{\theta \wedge \mathscr{D}\theta\}\,\mathrm{d}x$ the corresponding functional bi-vector. Then $\mathscr{D}$ is Hamiltonian if and only if*

$$\operatorname{pr} \mathbf{v}_{\mathscr{D}\theta}(\Theta_{\mathscr{D}}) = 0 \tag{1.16}$$

2. The Hamiltonian operators $\mathscr{D}$ and $\mathscr{E}$ are a Hamiltonian pair if and only if

$$\operatorname{pr} \mathbf{v}_{\mathscr{D}\theta}(\Theta_{\mathscr{E}}) + \operatorname{pr} \mathbf{v}_{\mathscr{E}\theta}(\Theta_{\mathscr{D}}) = 0 \tag{1.17}$$

3. Let $\mathscr{R} = \mathscr{E} \cdot \mathscr{D}^{-1}$ be the corresponding recursion operator and define $K_n = \mathscr{R} K_{n-1}$, then

$$m_t = K_n[m] = \mathscr{D}\delta\mathscr{H}_n = \mathscr{E}\delta\mathscr{H}_{n-1}$$

are also bi-Hamiltonian systems. This means that a bi-Hamiltonian system has infinitely many conserved quantities $\mathscr{H}_n$.

Assume two skew-adjoint differential operators $\mathscr{D}$ and $\mathscr{E}$ where $\mathscr{D} = \sum_K P_K[m]D_K$, then the following calculations show how one should interpret the expressions in (1.16) and (1.17)

$$\begin{aligned}\operatorname{pr}\mathbf{v}_{\mathscr{E}\theta}(\Theta_{\mathscr{D}}) &= \operatorname{pr}\mathbf{v}_{\mathscr{E}\theta}\left(\frac{1}{2}\int\{\theta\wedge\mathscr{D}\theta\}\,\mathrm{d}x\right)\\ &= \frac{1}{2}\operatorname{pr}\mathbf{v}_{\mathscr{E}\theta}\left(\int\{\sum_K(P_K\theta\wedge D_K\theta)\}\,\mathrm{d}x\right)\\ &= \frac{1}{2}\int\sum_K\{\operatorname{pr}\mathbf{v}_{\mathscr{E}\theta}(P_K)\wedge\theta\wedge D_K\theta\}\,\mathrm{d}x\end{aligned}\tag{1.18}$$

Now it is time to apply some of our newly acquired wisdom to the Camassa-Holm equation.

Proposition 1.4. *The Camassa-Holm equation* (1.1) *is bi-Hamiltonian. That is, it can be written on the form*

$$m_t = \mathscr{E}\delta\mathscr{H}_1[m] = \mathscr{D}\delta\mathscr{H}_2[m]\tag{1.19}$$

with Hamiltonians

$$\mathscr{H}_1[m] = \frac{1}{2}\int mu\,\mathrm{d}x, \qquad \mathscr{H}_2[m] = \frac{1}{2}\int(u^3+uu_x^2)\,\mathrm{d}x\tag{1.20}$$

and the corresponding Hamiltonian pair of operators

$$\mathscr{D} = -(D_x - D_x^3), \qquad \mathscr{E} = -(mD_x + D_xm)$$

Proof. First we must prove that $\mathscr{D}$ and $\mathscr{E}$ is a Hamiltonian pair. By inserting $\mathscr{D}$ and $\mathscr{E}$ into (1.15) one sees that they are both skew-adjoint, and by proposition 1.2 they are skew-symmetric.

To check that $\mathscr{D}$ and $\mathscr{E}$ is Hamiltonian, we apply (1.16)

$$\operatorname{pr}\mathbf{v}_{\mathscr{D}\theta}(\Theta_{\mathscr{D}}) = \frac{1}{2}\operatorname{pr}\mathbf{v}_{\mathscr{D}\theta}\left(\int\{\theta\wedge(\theta_{xxx}-\theta_x)\}\,\mathrm{d}x\right) = 0$$

trivially, since m does not appear inside the parentheses.

$$\begin{aligned}\operatorname{pr}\mathbf{v}_{\mathscr{E}\theta}(\Theta_{\mathscr{E}}) &= -\operatorname{pr}\mathbf{v}_{\mathscr{E}\theta}\left(\frac{1}{2}\int\{\theta\wedge(m\theta_x+(m\theta)_x)\}\,\mathrm{d}x\right)\\ &= -\operatorname{pr}\mathbf{v}_{\mathscr{E}\theta}\left(\frac{1}{2}\int\{2m\theta\wedge\theta_x+m_x\theta\wedge\theta\}\,\mathrm{d}x\right)\\ &= -\int\{(\mathscr{E}\theta\wedge\theta\wedge\theta_x)\}\,\mathrm{d}x\\ &= \int\{(2m\theta_x+m_x\theta)\wedge\theta\wedge\theta_x\}\,\mathrm{d}x\\ &= \int\{-2m\theta\wedge(\theta_x\wedge\theta_x)+m_x(\theta\wedge\theta)\wedge\theta_x\}\,\mathrm{d}x = 0\end{aligned}$$

Where integration by parts yields the penultimate equality, and we have used the fact that $\omega \wedge \omega = 0$.

By calculating (1.17) we see that they are in fact a Hamiltonian pair

$$\operatorname{pr} \mathbf{v}_{\mathscr{D}\theta}(\Theta_{\mathscr{E}}) + \operatorname{pr} \mathbf{v}_{\mathscr{E}\theta}(\Theta_{\mathscr{D}}) = -\operatorname{pr} \mathbf{v}_{\mathscr{D}\theta}\left(\int \{m\theta \wedge \theta_x\}\,\mathrm{d}x\right) + 0$$

Which follows from the previous calculations. Continue using the procedure (1.18).

$$\begin{aligned} &= -\int \{\mathscr{D}\theta \wedge \theta \wedge \theta_x\}\,\mathrm{d}x \\ &= \int \{\theta_x \wedge \theta \wedge \theta_x - \theta_{xxx} \wedge \theta \wedge \theta_x\}\,\mathrm{d}x \end{aligned}$$

Integrate both terms by parts to get:

$$\begin{aligned} &= \int \{-\theta \wedge \theta_x \wedge \theta_x + \theta_{xx} \wedge (\theta \wedge \theta_x)_x\}\,\mathrm{d}x \\ &= \int \{\theta_{xx} \wedge \theta_x \wedge \theta_x + \theta_{xx} \wedge \theta \wedge \theta_{xx}\}\,\mathrm{d}x = 0 \end{aligned}$$

Finally we need to show that (1.19) actually produces the Camassa-Holm equation (1.1). First we find the variational derivatives (1.13)

$$\begin{aligned} \left.\frac{\mathrm{d}}{\mathrm{d}\epsilon}\right|_{\epsilon=0} \mathscr{H}_1[m+\epsilon v] &= \left.\frac{\mathrm{d}}{\mathrm{d}\epsilon}\right|_{\epsilon=0} \int \frac{1}{2}(m+\epsilon v)(1-D_x^2)^{-1}(m+\epsilon v)\,\mathrm{d}x \\ &= \int (1-D_x^2)^{-1} m \cdot v\,\mathrm{d}x \end{aligned}$$

which implies $\delta\mathscr{H}_1[m] = (1-D_x^2)^{-1}m = u$.

$$\begin{aligned} \left.\frac{\mathrm{d}}{\mathrm{d}\epsilon}\right|_{\epsilon=0} \mathscr{H}_2[m+\epsilon v] &= \left.\frac{\mathrm{d}}{\mathrm{d}\epsilon}\right|_{\epsilon=0} \frac{1}{2}\left[\left(\left(1-D_x^2\right)^{-1}(m+\epsilon v)\right)^3\right. \\ &\qquad \left. + \left(1-D_x^2\right)^{-1}(m+\epsilon v)\left(D_x\left(1-D_x^2\right)^{-1}(m+\epsilon v)\right)^2\right]\mathrm{d}x \\ &= \int \left(1-D_x^2\right)^{-1}\left[\frac{3}{2}\left(\left(1-D_x^2\right)^{-1}m\right)^2 - \frac{1}{2}\left(D_x\left(1-D_x^2\right)^{-1}m\right)^2\right. \\ &\qquad \left. - \left(\left(1-D_x^2\right)^{-1}m\right)\left(D_x^2\left(1-D_x^2\right)^{-1}m\right)\right]\cdot v\,\mathrm{d}x \end{aligned}$$

which implies $\delta\mathscr{H}_2[m] = (1-D_x^2)^{-1}\left(\frac{3}{2}u^2 - \frac{1}{2}u_x^2 - uu_{xx}\right)$. We can then cal-

culate the expressions in (1.19)

$$\begin{aligned}
\mathscr{E}\delta\mathscr{H}_1[m] &= -(mD_x + D_x m)u \\
&= -mu_x - (mu)_x \\
&= -2mu_x - m_u \\
&= -3uu_x + 2u_x u_{xx} + uu_{xxx} \\
\mathscr{D}\delta\mathscr{H}_2[m] &= -(D_x - D_x^3)(1 - D_x^2)^{-1}\left(\frac{3}{2}u^2 - \frac{1}{2}u_x^2 - uu_{xx}\right) \\
&= -D_x\left(\frac{3}{2}u^2 - \frac{1}{2}u_x^2 - uu_{xx}\right) \\
&= -3uu_x + 2u_x u_{xx} + uu_{xxx}
\end{aligned}$$

Inserting these expressions into (1.19) gives (1.1). □

Using part 3 of theorem 1.3 one can calculate infinitely many conservation laws for the Camassa-Holm equation. In addition to $\mathscr{H}_1$ and $\mathscr{H}_2$, which we already know, one can use the relation $K_{n-1} = \mathscr{R}^{-1}K_n$ to find for example

$$\mathscr{H}_0 = \int m \, \mathrm{d}x$$

In [34] several of the conserved quantities are computed explicitly.

An alternative way to show that $\mathscr{H}$ is conserved is simply to calculate the time derivative and see that it vanishes. Assume that u is either periodic or decays at infinity such that the boundary terms vanish when integrating by parts

$$\begin{aligned}
\frac{\partial\mathscr{H}_1}{\partial t} &= \frac{1}{2}\int (mu)_t \, \mathrm{d}x \\
&= \frac{1}{2}\int (m_t u + mu_t) \, \mathrm{d}x \\
&= \frac{1}{2}\int (m_t u + uu_t - u_{xx}u_t) \, \mathrm{d}x \\
&= \frac{1}{2}\int (m_t u + uu_t - uu_{xxt}) \, \mathrm{d}x \\
&= \int m_t u \, \mathrm{d}x \\
&= \int (-2mu_x u - m_x u^2) \, \mathrm{d}x \\
&= \int (-2mu_x u + 2muu_x) \, \mathrm{d}x = 0
\end{aligned}$$

2 Numerical solutions of CH

We consider the periodic initial value problem

$$\begin{cases} u_t - u_{xxt} = -3uu_x + 2u_xu_{xx} + uu_{xxx}, & x \in [-\frac{a}{2}, \frac{a}{2}], t \geq 0 \\ u(-\frac{a}{2}, t) = u(\frac{a}{2}, t), & t \geq 0 \\ u(x, 0) = u_0(x) \end{cases}$$

In this chapter the available numerical methods are introduced. First we study the much used finite difference and spectral methods. Then we delve into the modern research of multisymplectic methods, before we introduce a new class of methods based on the Euler equation. At last we look into multipeakon methods, which differ somewhat from the other methods. Some of the methods are modified to yield increased performance. Some numerical tests will be performed on each method. We will in this chapter mostly be interested in the qualitative behaviour of the methods, especially studying peakon-antipeakon collisions. In chapter 3 a more objective comparison of the methods will be done.

There are some methods not featured in this thesis that are still worth mentioning. The method of adaptive upwinding [4] and the local discontinuous Galerkin method [44] are omitted because they are rather comprehensive to implement. The local discontinuous Galerkin method looks promising, but the research is very recent and the authors have not implemented it for Matlab yet. A third class of new methods using moving frames and the theory of multi-space is introduced in [33]. It applies a method called invariantisation to existing numerical methods, increasing the structure preserving properties. Unfortunately the method is not yet extended to partial differential equations, however this is the subject of current research.

2.1 Finite difference methods

The well-known finite difference methods approximate the PDE by introducing forward and backward difference operators to the discretised variable $u^n = (u_1, \dots, u_n)^T$

$$(\delta^+ u^n)_i = \frac{1}{h}(u_i - u_{i-1}) \quad \text{and} \quad (\delta^- u^n)_i = \frac{1}{h}(u_{i+1} - u_i) \tag{2.1}$$

and the central difference operator

$$\delta = \frac{1}{2}(\delta^+ + \delta^-)$$

Holden and Raynaud [23] prove that the following semidiscretised finite difference scheme converge

$$\begin{aligned} m_t^n &= -\delta^-(m^n u^n) - m^n \delta u^n \\ m^t &= u^n - \delta^- \delta^+ u^n \end{aligned} \tag{2.2}$$

The occurence of δ^- in the first line of (2.2) means that this is an upwind method. That is, the information is taken from the side where the wave comes from. However, we want our schemes to handle antipeakons as well. One possible remedy is to replace the one-sided difference operator with a central operator. This gives the scheme

$$\begin{aligned} m_t^n &= -\delta(m^n u^n) - m^n \delta u^n \\ m^t &= u^n - \delta^- \delta^+ u^n \end{aligned} \tag{2.3}$$

This scheme is briefly considered in [23], but claimed to produce oscillations. These oscillations make it impossible to prove convergence, but in some situations this scheme will still perform better than (2.2). There is a way to make the scheme (2.2) be able to handle antipeakons while still preserving the damping effect which is necessary to avoid oscillations. We essentially want an upwind method when $u > 0$ and a downwind method when $u < 0$. Then the information will be taken from the side where the wave comes from. The trick is found in [13] and consists of replacing $\delta^- u$ with $\delta^-(u \vee 0) + \delta^+(u \wedge 0)$ where we use the following notation

$$a \vee 0 = \max\{a, 0\} = \frac{a + |a|}{2}, \qquad a \wedge 0 = \min\{a, 0\} = \frac{a - |a|}{2}$$

Applying this trick to (2.2) yields the modified scheme

$$\begin{aligned} m_t^n &= -\delta^-(m^n (u \vee 0)^n) - \delta^+(m^n (u \wedge 0)^n) - m^n \delta u^n \\ m^t &= u^n - \delta^- \delta^+ u^n \end{aligned} \tag{2.4}$$

When calculating (2.3) one needs to go back and forth between u^n and m^n. Given u^n, we get

$$m^n = Lu^n = (I - \delta^-\delta^+)u^n \tag{2.5}$$

which in practice is a matrix multiplying a vector. Going the other way, however, is not as simple. One could solve the inverse problem

$$u^n = (I - \delta^-\delta^+)^{-1}m^n$$

This means solving a linear system of equations for each time step. A faster method which utilizes the FFT is presented in [23]; introduce the vector χ

$$\chi_i = \begin{cases} 1 & \text{when } i = 0 \\ 0 & \text{elsewhere} \end{cases}$$

Then it is enough to find a solution g of

$$Lg = \chi \tag{2.6}$$

where L is defined in (2.5) and g decays at infinity. Then $L^{-1}m$ is given by

$$L^{-1}m_i = \sum_j g_{i-j}m_j$$

Inserting (2.1), (2.5) and $\frac{1}{h} = n$ into (2.6) gives for i nonzero

$$g_i - n^2(g_{i+1} - 2g_i + g_{i-1}) = 0 \tag{2.7}$$

This is a difference equation, and we try the following solution

$$g_i = c\mathrm{e}^{ki}$$

where c is a constant. (2.7) then becomes

$$\begin{aligned} c\mathrm{e}^{ki} - n^2(c\mathrm{e}^{k(i+1)} - 2c\mathrm{e}^{ki} + c\mathrm{e}^{k(i-1)}) &= 0 \\ -n^2\mathrm{e}^{2k} + (1 + 2n^2)\mathrm{e}^k - n^2 &= 0 \end{aligned}$$

This is simply a second degree algebraic equation which we solve to get

$$\mathrm{e}^{k_1} = \frac{1 + 2n^2 + \sqrt{1 + 4n^2}}{2n^2} \text{ and } \mathrm{e}^{k_2} = \frac{1 + 2n^2 - \sqrt{1 + 4n^2}}{2n^2}$$

We know that in general the two solutions x_1 and x_2 of $ax^2 + bx + c = 0$ obey $\frac{x_1}{x_2} = \frac{a}{c}$. With $a = c = -n^2$ we must have $\mathrm{e}^{k_1}\mathrm{e}^{k_2} = 1$, that is $k_1 = -k_2 = k$. Thus we take g on the form

$$g_i = c\mathrm{e}^{-k|i|}$$

so that g decays at infinity. Recall that $(Lg)_0 = 1$ which means

$$\begin{aligned} g_0 - n^2(g_1 - 2g_0 + g_{-1}) &= 1 \\ c - n^2(c\mathrm{e}^{-k} - 2c + c\mathrm{e}^{-k}) &= 1 \end{aligned}$$

which yields the constant

$$c = \frac{1}{1 + 2n^2(1 - \mathrm{e}^{-k})}$$

The periodized version of g is

$$g_i^p = \sum_k g_{i+kn} = c\frac{\mathrm{e}^{-ki} + \mathrm{e}^{k(i-n)}}{1 - \mathrm{e}^{kn}}$$

for $i \in \{0, \dots, n-1\}$. The inverse of L on the set of periodic sequences is then given by

$$u_i = L^{-1}m_i = \sum_{j=0}^{n-1} g_{i-j}^p m_i = \frac{c}{1 - \mathrm{e}^{-kn}} \sum_{j=0}^{n-1} (\mathrm{e}^{-k(i-j)} + \mathrm{e}^{-k(i-j-n)})m_j$$

Luckily this discrete convolution can be evaluated efficiently using the FFT algorithm, here denoted by $\mathcal{F}$

$$u = \mathcal{F}^{-1}(\mathcal{F}[g] \cdot \mathcal{F}[m])$$

The final finite difference scheme we will consider is that found in [13]. It is based on the elliptic-hyperbolic formulation (1.3) and is convergent and handles antipeakons

$$\begin{aligned} \frac{\mathrm{d}}{\mathrm{d}t}u_{j+\frac{1}{2}} + (u_{j+\frac{1}{2}} \vee 0)\delta^- u_{j+\frac{1}{2}} + (u_{j+\frac{1}{2}} \wedge 0)\delta^+ u_{j+\frac{1}{2}} + \delta^+ P_j &= 0 \\ P_j - \delta^-\delta^+ P_j = (u_{j+\frac{1}{2}} \vee 0)^2 + (u_{j-\frac{1}{2}} \wedge 0)^2 + \frac{1}{2}(\delta^- u_{j+\frac{1}{2}})^2 & \end{aligned} \tag{2.8}$$

Note that the discretisation of P is shifted one half-cell compared that of u.

Since all the schemes above are semi-discrete, we need to solve the resulting ODE. [23] integrates in time using the explicit Euler method, we will be using Matlabs ode45. There is not much difference between the two, but the adaptive step size and higher order of ode45 generally give better and faster results. The figures 6 and 7 compare the performance of some of the finite difference schemes on different initial conditions, while figure 8 and 9 show how the methods handle peakon-antipeakon.

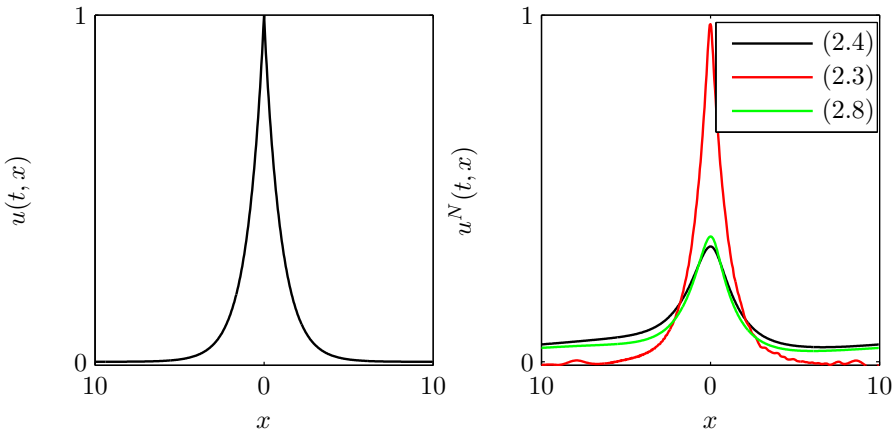

Figure 6: The figure to the left shows the initial peakon at $t = 0$ while the figure to the right shows the approximated solution with $n = 512$ at $t = 100$ (5 periods) approximated with three different finite difference methods. The peakons are shifted to the center for comparison. Clearly the central difference scheme (2.3) produces the most accurate solution, although it has some minor oscillations. The other two schemes suffer from the damping effect which causes the peakon height to decrease considerably.

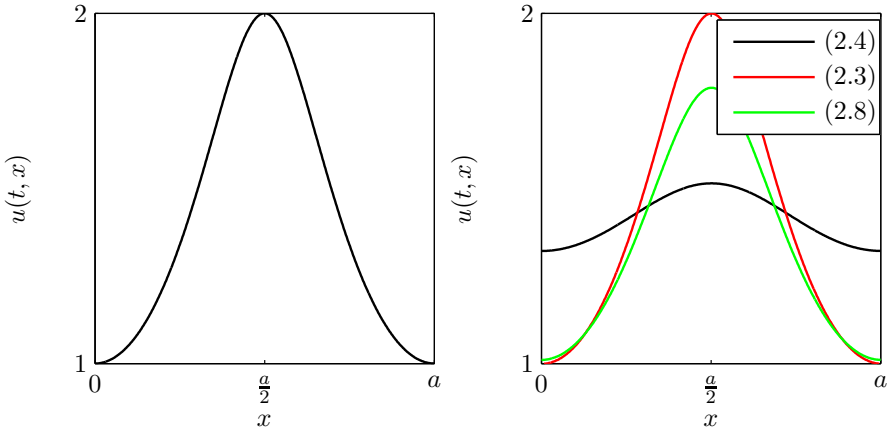

Figure 7: The figure to the left shows the initial smooth solution given by (1.7) at $t = 0$ while the figure to the right shows the approximated solution with $n = 512$ at $t = 100$ for the three finite difference methods. The solutions are shifted to the center for comparison. All the methods perform better than for the non-smooth initial condition, however again we see that the central difference scheme (2.3) outperforms the other two. The scheme (2.8) seems to be doing better than (2.4).

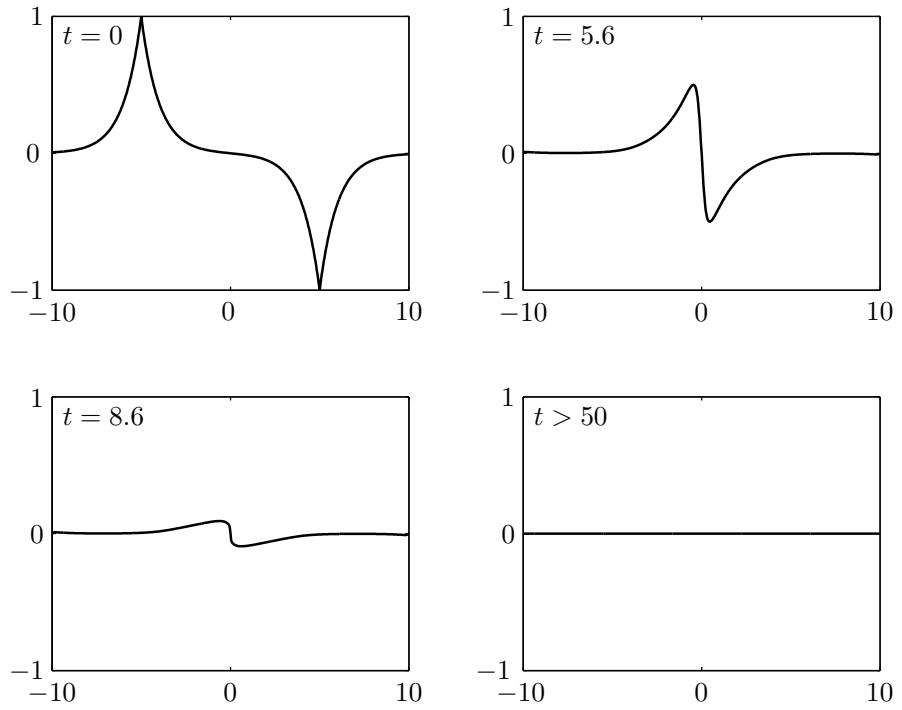

Figure 8: Peakon-antipeakon initial conditions in the first figure, then approximated solutions calculated with the modified version of Holden and Raynaud's method (2.4) (the method (2.8) behaves similarly). The solution is dissipative, which means that the peakons will not re-emerge after the collision.

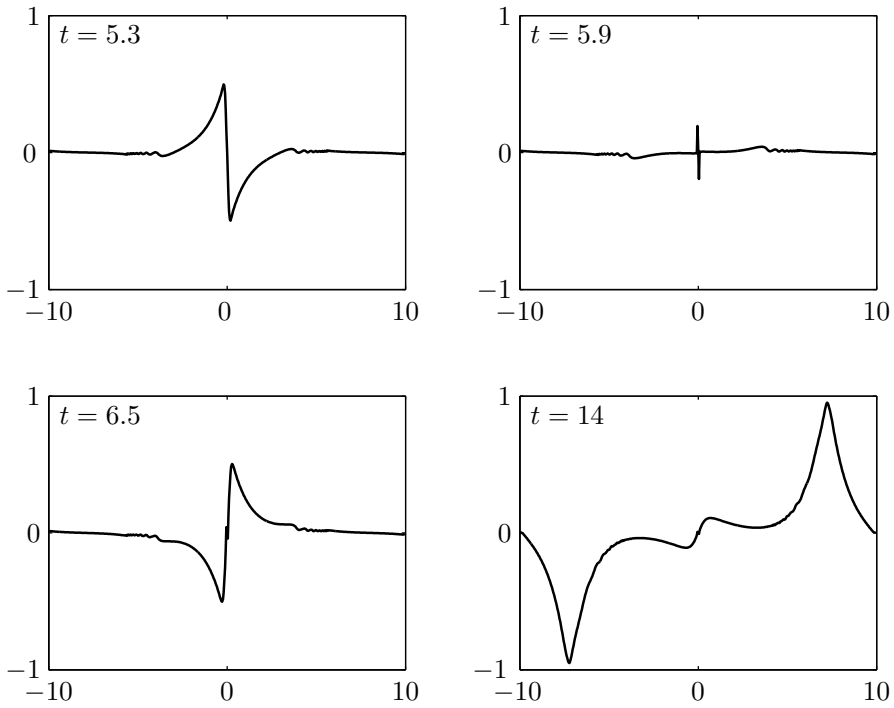

Figure 9: The initial condition is the same as in 8, however here we have used the scheme (2.3). The solution never quite vanish, and the peakons re-emerge after the collison. From the last figure, however, we see that the solution develops a wave around $x = 0$ which does not coincide with the exact solution. This wave will not decrease for higher n or lower time steps. Thus method (2.4) will not converge after a peakon-antipeakon collision.

2.2 Spectral methods

Following [30] we derive a spectral projection of the CH equation. First (1.1) is written on the form

$$u_t + \frac{1}{2}(u^2)_x + K(u^2 + \frac{1}{2}(u_x)^2) = 0$$

with the operator

$$K = \frac{\partial_x}{1 - \partial_x^2}$$

Since the solution is periodic we can do a discrete Fourier transform of the space-discretised u^N

$$\hat{u}^N = \mathcal{F}(u^N) = \sum_{k=-\frac{N}{2}}^{\frac{N}{2}-1} u^N(k,t)\mathrm{e}^{-\mathrm{i}kx}$$

Now differentiation simply becomes

$$\delta_x u^N(k) = \mathcal{F}^{-1}(\mathrm{i}k\hat{u}^N)(k)$$

where $u^N(k)$ denotes the k'th element of the vector u^N. This gives the following system of ordinary differential equations

$$\frac{\mathrm{d}}{\mathrm{d}t}\hat{u}^N(k) + \frac{\mathrm{i}k}{2}\mathcal{F}\left(\left(\mathcal{F}^{-1}\hat{u}^N\right)^2\right)(k) + \frac{\mathrm{i}k}{1+k^2}\mathcal{F}\left[\left(\mathcal{F}^{-1}\hat{u}^N\right)^2 + \frac{1}{2}\left(\mathcal{F}^{-1}(\mathrm{i}k\hat{u}^N)\right)^2\right](k) = 0 \quad (2.9)$$

for $-\frac{N}{2} \le k \le \frac{N}{2} - 1$. The initial condition becomes $\hat{u}^N(k,0) = \mathcal{F}u^N(k,0)$.

The evaluation of the discrete Fourier transform is done by the very effective FFT algorithm. To avoid aliasing errors caused by the FFT one applies the 2/3-rule [11]. The 2/3-rule works by cutting of the highest third of the frequencies in the nonlinear terms in (2.9). This gives the new system

$$\frac{\mathrm{d}}{\mathrm{d}t}\hat{u}^N(k) + \frac{\mathrm{i}k}{2}\mathcal{F}\left(\left(\mathcal{F}^{-1}\hat{u}_c^N\right)^2\right)(k) + \frac{\mathrm{i}k}{1+k^2}\mathcal{F}\left[\left(\mathcal{F}^{-1}\hat{u}_c^N\right)^2 + \frac{1}{2}\left(\mathcal{F}^{-1}(\mathrm{i}k\hat{u}_c^N)\right)^2\right](k) = 0 \quad (2.10)$$

where we introduced

$$\hat{u}_c^N(k) = \begin{cases} \hat{u}^N(k) & \text{if } -\frac{2N}{3} - 1 \le k \le \frac{2N}{3} \\ 0 & \text{otherwise} \end{cases}$$

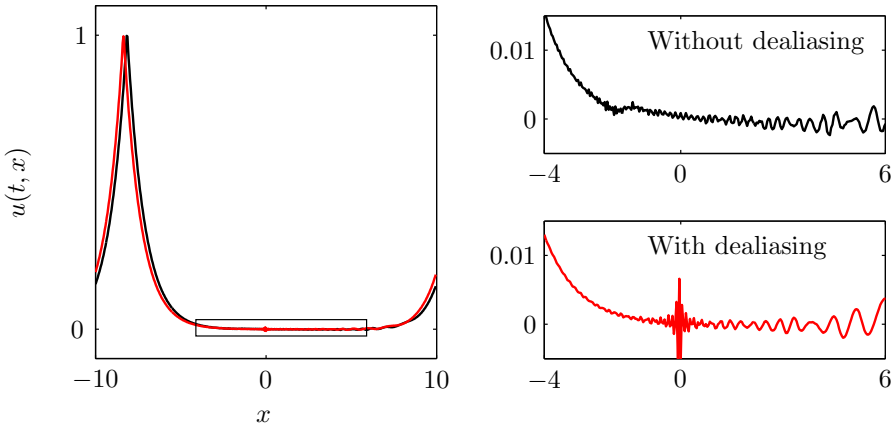

Figure 10: The figure to the left shows the numerical solution of a peakon at $t = 32$ with $n = 512$, with and withouth dealiasing. The magnified figures to the right indicate that although the solution in general becomes smoother when applying the 2/3-rule, it produces larger oscillations at $x = 0$. However, for non-smooth initial conditions the numerical solution is more stable when using dealiasing.

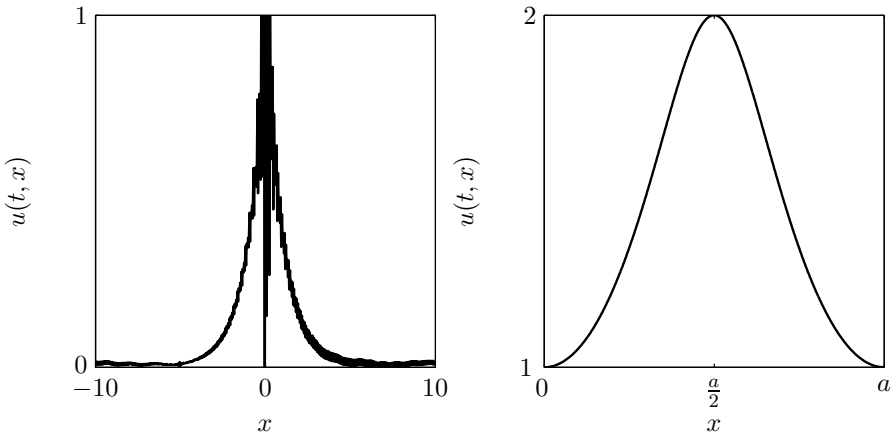

Figure 11: The numerical solution of a non-smooth peakon and a smooth wave. These are calculated at $t = 85$ and $t = 100$ respectively and shifted to the centre. The oscillations in the peakon case become increasingly severe, and it is clear that a spectral method is unsuitable for non-smooth initial conditions. Interestingly, the scheme without the 2/3-rule applied breaks down at $t = 66$ while the dealiased scheme breaks down at $t = 138$ in the peakon case, indicating the advantage of dealiasing. The spectral method seems to give accurate results in the smooth case.

2.3 Multisymplectic

A PDE is said to be multisymplectic if it can be written as

$$\mathbf{M}z_t + \mathbf{K}z_x = \nabla_z S(z) \tag{2.11}$$

with phase space variable $z(x,t) \in \mathbb{R}^d$. The matrices $\mathbf{M}, \mathbf{K} \in \mathbb{R}^{d\times d}$ are skew-symmetric and $S : \mathbb{R}^d \mapsto \mathbb{R}$ is a scalar-valued smooth function. Multisymplectic integration is still to be considered a new and not settled field of research, it can therefore be hard to find introductory texts on the subject. The interested reader should see the phd thesis of Brian E. Moore. In this paper we will be following the methodology of Bridges and Reich [7, 8, 41]. Alternatively, one may be able to start from first-order field theory defined by a Lagrangian. This will not be pursued here, but is the approach by Marsden et.al. [36, 38].

Proposition 2.1. *The Camassa-Holm equation* (1.1) *can be written on the multisymplectic form* (2.11) *with the phase space variable:* $z = \begin{bmatrix} u & \varphi & \omega & v & \nu \end{bmatrix}^T$ *and the function* $S(z) = -\omega u - \frac{1}{2}u^3 - \frac{1}{2}u\nu^2 + \nu v$. *The two matrices are given as:*

$$\mathbf{M} = \begin{bmatrix} 0 & \frac{1}{2} & 0 & 0 & -\frac{1}{2} \\ -\frac{1}{2} & 0 & 0 & 0 & 0 \\ 0 & 0 & 0 & 0 & 0 \\ 0 & 0 & 0 & 0 & 0 \\ \frac{1}{2} & 0 & 0 & 0 & 0 \end{bmatrix} \qquad \mathbf{K} = \begin{bmatrix} 0 & 0 & 0 & -1 & 0 \\ 0 & 0 & 1 & 0 & 0 \\ 0 & -1 & 0 & 0 & 0 \\ 1 & 0 & 0 & 0 & 0 \\ 0 & 0 & 0 & 0 & 0 \end{bmatrix}$$

Proof. The five equations are

$$\begin{aligned} \frac{1}{2}\varphi_t - \frac{1}{2}\nu_t - v_x &= -\omega - \frac{3}{2}u^2 - \frac{1}{2}\nu^2 \\ -\frac{1}{2}u_t + \omega_x &= 0 \\ -\varphi_x &= -u \\ u_x &= \nu \\ \frac{1}{2}u_t &= -u\nu + v \end{aligned}$$

Insert the last three equations into the first wherever possible

$$\frac{1}{2}\varphi_t - \frac{1}{2}u_{xt} - (uu_x)_x = -\omega - \frac{3}{2}u^2 - \frac{1}{2}u_x^2$$

Which means:

$$\omega = -\frac{3}{2}u^2 + \frac{1}{2}u_x^2 - \frac{1}{2}\varphi_t + u_{xt} + uu_{xx}$$

Insert ω_x and $\varphi_{xt} = u_t$ into the second equation

$$-\frac{1}{2}u_t - 3uu_x + u_x u_{xx} - \frac{1}{2}u_t + u_{xxt} + u_x u_{xx} + uu_{xxx} = 0$$
$$u_t - u_{xxt} + 3uu_x - 2u_x u_{xx} - uu_{xxx} = 0$$

Which is the desired equation. □

The multisymplectic structure is given by the two 2-forms

$$\omega = \mathbf{d}z \wedge \mathbf{M}\mathbf{d}z \qquad \text{and} \qquad \kappa = \mathbf{d}z \wedge \mathbf{K}\mathbf{d}z$$

Before we proceed to the proof of conservation of multisymplecticity, we need to prove a property of the wedge product:

Lemma 2.2. *The identity:*

$$\mathbf{d}a \wedge \mathbf{A}\mathbf{d}b = \mathbf{A}^T\mathbf{d}a \wedge \mathbf{d}b$$

is satisfied by the wedge product for any real $d \times d$ matrix $\mathbf{A}$.

Proof. Suppose $\mathbf{d}a = (\mathrm{d}a_1, \ldots, \mathrm{d}a_d)^T$, $\mathbf{d}b = (\mathrm{d}b_1, \ldots, \mathrm{d}b_d)^T$ and $\mathbf{A} = \{A_{ij}\}$. Then:

$$\begin{aligned}
\mathbf{d}a \wedge \mathbf{A}\mathbf{d}b &= \mathrm{d}a_1 \wedge (A_{11}\mathrm{d}b_1 + \cdots + A_{1d}\mathrm{d}b_d) + \ldots \\
&\quad \cdots + \mathrm{d}a_d \wedge (A_{d1}\mathrm{d}b_1 + \cdots + A_{dd}\mathrm{d}b_d) \\
&= A_{11}\mathrm{d}a_1 \wedge \mathrm{d}b_1 + \cdots + A_{1d}\mathrm{d}a_1 \wedge \mathrm{d}b_d + \ldots \\
&\quad \cdots + A_{d1}\mathrm{d}a_d \wedge \mathrm{d}b_1 + \cdots + A_{dd}\mathrm{d}a_d \wedge \mathrm{d}b_d \\
&= (A_{11}\mathrm{d}a_1 + \cdots + A_{d1}\mathrm{d}a_d) \wedge \mathrm{d}b_1 + \ldots \\
&\quad \cdots + (A_{1d}\mathrm{d}a_1 + \cdots + A_{dd}\mathrm{d}a_d) \wedge \mathrm{d}b_d \\
&= \mathbf{A}^T\mathbf{d}a \wedge \mathbf{d}b
\end{aligned}$$

□

For $\mathbf{A}$ symmetric, this immediately implies the identity

$$\mathbf{d}a \wedge \mathbf{A}\mathbf{d}b = -\mathbf{d}b \wedge \mathbf{A}\mathbf{d}a$$

which also means that:

$$\mathbf{d}a \wedge \mathbf{A}\mathbf{d}a = 0$$

We use this in the proof of the following proposition.

Proposition 2.3 (Conservation of multisymplecticity)**.**

$$\omega_t + \kappa_x = 0$$

Proof.

$$\begin{aligned}\omega_t + \kappa_x &= \mathbf{d}z_t \wedge \mathbf{M}\mathbf{d}z + \mathbf{d}z \wedge \mathbf{M}\mathbf{d}z_t + \mathbf{d}z_x \wedge \mathbf{K}\mathbf{d}z\mathbf{d}z \wedge \mathbf{K}\mathbf{d}z_x \\ &= -(\mathbf{M}\mathbf{d}z_t + \mathbf{K}\mathbf{d}z_x) \wedge \mathbf{d}z + \mathbf{d}z \wedge (\mathbf{M}\mathbf{d}z_t + \mathbf{K}\mathbf{d}z_x)\end{aligned}$$

Use the variational equation associated with (2.11): $\mathbf{K}\mathbf{d}z_t + \mathbf{M}\mathbf{d}z_x = S_{zz}\mathbf{d}z$.

$$= -S_{zz}\mathbf{d}z \wedge \mathbf{d}z + \mathbf{d}z \wedge S_{zz}\mathbf{d}z = 0$$

Where we have used Leibniz' rule, the lemma 2.2 and the fact that the Hessian S_{zz} is symmetric. □

This means that at each point (x, t) the multisymplectic structure is conserved, i.e. a local property. This leads to local conservation laws for energy and momentum. By integrating these with suitable boundary conditions one gets global conservation laws. Conservation of energy and momentum is an advantageous quality and we wish to preserve this property in a numerical scheme. A multisymplectic integrator is a map which preserves a discrete version of the multisymplectic structure

$$\mathbf{M}\delta_t^{n,i} z^{n,i} + \mathbf{K}\delta_x^{n,i} z^{n,i} = (\nabla_z S(z^{n,i}))^{n,i}$$

such that

$$\delta_t^{n,i}\omega^{n,i} + \delta_x^{n,i}\kappa^{n,i} = 0 \tag{2.12}$$

Here we use the notation $z^{n,i}$ to denote a numerical approximation of $z(x_n, t_i)$ and $\delta_t^{n,i}$ and $\delta_x^{n,i}$ are difference operators. An example is the Euler box scheme where a symplectic Euler discretisation is applied to each independent variable

$$\mathbf{M}_+\delta_t^+ z^{n,i} + \mathbf{M}_-\delta_t^- z^{n,i} + \mathbf{K}_+\delta_x^+ z^{n,i} + \mathbf{L}_-\delta_x^- z^{n,i} = \nabla_z S(z^{n,i}) \tag{2.13}$$

Where

$$\mathbf{K} = \mathbf{K}_+ + \mathbf{K}_- \qquad \text{and} \qquad \mathbf{M} = \mathbf{M}_+ + \mathbf{M}_-$$

with

$$\mathbf{K}_+^T = -\mathbf{K}_- \qquad \text{and} \qquad \mathbf{M}_+^T = -\mathbf{L}_- \tag{2.14}$$

Using forward and backward differences, define discrete approximations to z_x by

$$\delta_x^+ z^{n,i} = \frac{z^{n+1,i} - z^{n,i}}{\Delta x} \qquad \text{and} \qquad \delta_x^- z^{n,i} = \frac{z^{n,i} - z^{n-1,i}}{\Delta x} \tag{2.15}$$

and discrete approximations to z_t by:

$$\delta_t^+ z^{n,i} = \frac{z^{n,i+1} - z^{n,i}}{\Delta t} \qquad \text{and} \qquad \delta_t^- z^{n,i} = \frac{z^{n,i} - z^{n,i-1}}{\Delta t} \tag{2.16}$$

where $\Delta x = x_n - x_{n-1}$ and $\Delta t = t_n - t_{n-1}$. Other examples of symplectic integrators include the Preissman box scheme and the explicit midpoint scheme. For the Euler box scheme to be a multisymplectic integrator it has to satisfy (2.12). In fact:

Proposition 2.4. *The Euler box scheme given by* (2.13) *satisfies a discrete multisymplectic conservation law:*

$$\delta_t^+ \omega^{n,i} + \delta_x^+ \kappa^{n,i} = 0 \tag{2.17}$$

where

$$\omega^{n,i} = \mathbf{d}z^{n,i-1} \wedge \mathbf{K}_+ \mathbf{d}z^{n,i} \qquad \text{and} \qquad \kappa^{n,i} = \mathbf{d}z^{n-1,i} \wedge \mathbf{M}_+ \mathbf{d}z^{n,i}$$

Proof. Consider the discrete variational equation

$$\mathbf{K}_+ \delta_t^+ \mathbf{d}z^{n,i} + \mathbf{K}_- \delta_t^- \mathbf{d}z^{z,i} + \mathbf{M}_+ \delta_x^+ \mathbf{d}z^{z,i} + \mathbf{M}_- \delta_x^- \mathbf{d}z^{z,i} = S_{zz}(z^{n,i}) \mathbf{d}z^{z,i}$$

Take the wedge product with $\mathbf{d}z^{n,i}$, the first two terms become

$$\begin{aligned} \mathbf{d}z^{n,i} \wedge \mathbf{K}_+ \delta_t^+ \mathbf{d}z^{n,i} + \mathbf{d}z^{n,i} \wedge \mathbf{K}_- \delta_t^- \mathbf{d}z^{z,i} \\ = \mathbf{d}z^{n,i} \wedge \mathbf{K}_+ \delta_t^+ \mathbf{d}z^{n,i} - \mathbf{K}_+ \mathbf{d}z^{n,i} \wedge \delta_t^- \mathbf{d}z^{z,i} \end{aligned}$$

Where we have used lemma 2.2 and the skew-symmetry (2.14). Use the skew-symmetry of the wedge product to get

$$\begin{aligned} &= \mathbf{d}z^{n,i} \wedge \mathbf{K}_+ \delta_t^+ \mathbf{d}z^{n,i} + \delta_t^- \mathbf{d}z^{n,i} \wedge \mathbf{K}_+ \mathbf{d}z^{z,i} \\ &= \frac{1}{\Delta t} \left(\mathbf{d}z^{n,i} \wedge \mathbf{K}_+ \mathbf{d}z^{n,i+1} - \mathbf{d}z^{n,i-1} \wedge \mathbf{K}_+ \mathbf{d}z^{n,i} \right) \\ &= \delta_t^+ (\mathbf{d}z^{n,i-i} \wedge \mathbf{K}_+ \mathbf{d}z^{n,i}) \end{aligned}$$

Doing the same for the next two terms yields

$$\mathbf{d}z^{n,i} \wedge \mathbf{M}_+ \delta_x^+ \mathbf{d}z^{z,i} + \mathbf{d}z^{n,i} \wedge \mathbf{M}_- \delta_x^- \mathbf{d}z^{z,i} = \delta_x^+ (\mathbf{d}z^{n-1,i} \wedge \mathbf{M}_+ \mathbf{d}z^{n,i})$$

From lemma 2.2 we see that

$$\mathbf{d}z^{n,i} \wedge S_{zz}(z^{n,i}) \mathbf{d}z^{n,i} = 0$$

since S_{zz} is symmetric. This implies (2.17). □

The Euler box scheme does not in general conserve the energy and momentum. However, there are semi-discrete conservation laws that are preserved exactly [39].

Figure 12 shows a peakon and a smooth solution approximated with the Euler box scheme applied to an 8×8 multisymplectic formulation [14]. The peakon initial condition develops oscillations which eventually lead to blowup, while the scheme performs well on the smooth initial condition. In figure 13 one sees that the multisymplectic method handles peakon-antipeakon collisions.

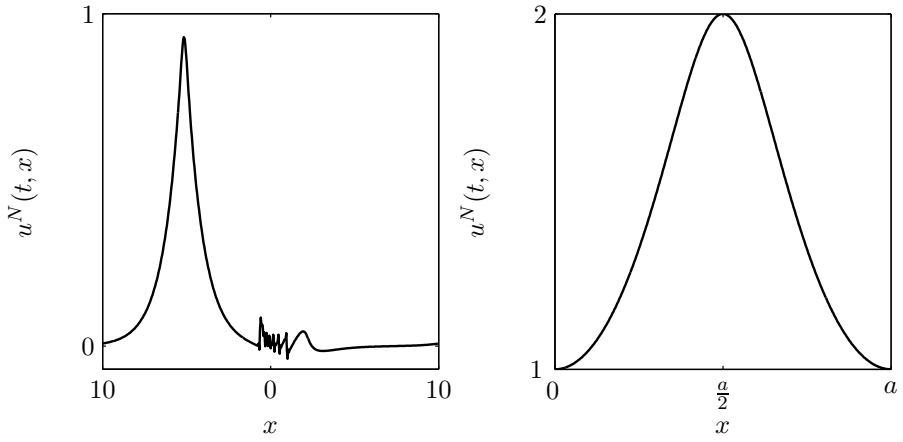

Figure 12: To the left: the initial condition is a peakon at $x = 0$, this is the approximated solution at $t = 15$ with $N = 512$. The smooth solution to the left at $t = 100$ is close to the exact solution.

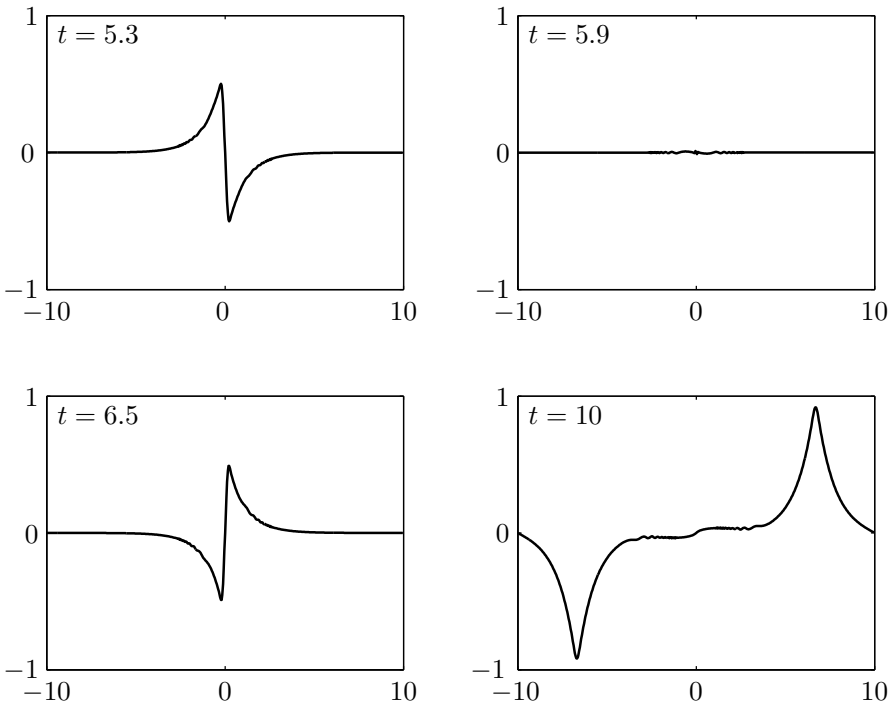

Figure 13: A Peakon-antipeakon collision. The multisymplectic method produces the conservative solution, and the two peakons remerge after the solution. Compare to figure 9.

2.4 Lie group integrator with frozen coefficients

Recall from section 1.1 that a whole class of equations, among them the Camassa-Holm equation, can be written as the nonlinear PDE

$$\frac{\mathrm{d}m}{\mathrm{d}t} = \mathrm{ad}_u^* m, \qquad u = A^{-1}m \tag{2.18}$$

A possible way of solving it numerically is to freeze u at a given time, that is $\bar{u} = A^{-1}\bar{m}$. Then the problem becomes a linear PDE in the variable $m(x,t)$

$$m_t = \mathrm{ad}^*_{A^{-1}\bar{m}} m \tag{2.19}$$

having formally the solution:

$$m(t) = \exp(t\mathrm{ad}^*_{A^{-1}\bar{m}}\bar{m})m(0) \tag{2.20}$$

The solution to (2.20) will soon deviate from the exact solution since $\bar{u}$ is frozen at $t = 0$. A possible remedy is to move only a small distance and then recalculate $\bar{u}$. Going back and forth between calculating $\bar{u} = A^{-1}\bar{m}$ and solving (2.20) will thus be a viable method of approximating (2.18). Lie group integrators generalize this approach by considering the ODE

$$\dot{m} = F(m) \cdot m, \qquad F(m) \in \mathfrak{g} \tag{2.21}$$

There are several types of Lie group integrators, for example Crouch-Grossman methods, Magnus methods and Runge-Kutta-Munthe-Kaas methods (see [27] for a thorough review of some of these methods). The advantage of these methods is that the solution will stay on the Lie group. We will be considering the commutator-free methods of Celledoni, Marthinsen and Owren [12]. In the case of the Euler equation we have $F(m) \cdot m = \mathrm{ad}^*_{A^{-1}m} m$, and the CFREE methods will be on the form given by the following algorithm.

Algorithm 1 Time stepping with a Lie group integrator

Assume m_i is given from the previous time step.
for $r = 1$ to s **do**
  $M_r = \exp(\sum_k \alpha^k_{rJ} U_k) \cdots \exp(\sum_k \alpha^k_{r1} U_k) m_i$
  $U_r = hA^{-1}M_r$
end for
$m_{i+1} = \exp(\sum_k \beta^k_J U_k) \cdots \exp(\sum_k \beta^k_1 U_k) m_i$

Where $h = t_{k+1} - t_k$ is the step-size and the coefficients α and β are usually given in a Butcher tableau, see table 1, two common examples are given in table 2.

To apply the Lie group integrators to the Camassa-Holm equation we need to write it on the form (2.21). Freeze u at a given time $\bar{t}$, $\bar{u}(x) = u(x,\bar{t})$,

$$
\begin{array}{c|cccc}
0 & 0 & & & \\
c_2 & \alpha_{2j}^1 & & & \\
\vdots & \vdots & \ddots & & \\
c_s & \alpha_{sj}^1 & \dots & \alpha_{sj}^{s-1} & 0 \\
\hline
 & \beta_j^1 & \dots & \beta_j^{s-1} & \beta_j^s
\end{array}
\qquad \forall j = 1 \dots J
$$

Table 1: Butcher tableau for the Lie group integrators given in algorithm 1. Notice that $\alpha_{rj}^k = 0$ for all $k \geq r$ for the method to be explicit. As for Runge-Kutta methods we have $c_r = \sum_{k,j} \alpha_{r,j}^k$.

$$
\begin{array}{c|cc}
0 & 0 & \\
1 & 1 & \\
\hline
 & \frac{1}{2} & \frac{1}{2}
\end{array}
\qquad
\begin{array}{c|cccc}
0 & 0 & & & \\
\frac{1}{2} & \frac{1}{2} & & & \\
\frac{1}{2} & 0 & \frac{1}{2} & & \\
1 & \frac{1}{2} & 0 & 0 & \\
 & -\frac{1}{2} & 0 & 1 & \\
\hline
 & \frac{1}{12} & \frac{1}{6} & \frac{1}{6} & \frac{1}{4} \\
 & \frac{1}{4} & \frac{1}{6} & \frac{1}{6} & -\frac{1}{12}
\end{array}
$$

Table 2: The coefficients of the second order scheme CFREE2 and the fourth order scheme CFREE4.

we then regard $\bar{u}$ and $\bar{u}_x$ as functions of x only. Simplify the CH equation by rewriting (1.2)

$$m_t(x,t) = a(x)m(x,t) - b(x)m_x(x,t) \tag{2.22}$$

Since the solution is periodic we can do a discrete Fourier transform of the space-discretised variables u^N, m^N, a^N and b^N

$$
\begin{aligned}
m^N(x,t) &= \frac{1}{N}\sum_k \hat{m}_k(t)\mathrm{e}^{\mathrm{i}kx} \\
a^N(x) &= \frac{1}{N}\sum_\ell \hat{a}_\ell \mathrm{e}^{\mathrm{i}\ell x} \\
b^N(x) &= \frac{1}{N}\sum_\ell \hat{b}_\ell \mathrm{e}^{\mathrm{i}\ell x}
\end{aligned}
$$

Assume that the Fourerier coefficients $\hat{m}_k$, $\hat{a}_\ell$ and $\hat{b}_\ell$ are periodic, they are thus defined for all $k, \ell \in \mathbb{Z}$. The summations must therefore be over N consecutive coefficients, it does not matter which. Henceforth we will apply the convention $k = -\frac{N}{2} \dots \frac{N}{2} - 1$. Insert the Fourier transformed expression into (2.22) and use the differentiation rules from section 2.2

$$\frac{1}{N}\sum_k \dot{\hat{m}}_k \mathrm{e}^{\mathrm{i}kx} = \frac{1}{N^2}\sum_{k,\ell} \hat{a}_\ell \hat{m}_k \mathrm{e}^{\mathrm{i}(k+\ell)x} + \frac{1}{N^2}\sum_{k,\ell} \mathrm{i}k\hat{b}_\ell \hat{m}_k \mathrm{e}^{\mathrm{i}(k+\ell)x}$$

Write $q = k+\ell$. Because of the periodicity we have $\hat{a}_{\ell+N} = \hat{a}_\ell$ and $\hat{b}_{\ell+N} = \hat{b}_\ell$, which yields

$$= \frac{1}{N^2}\sum_q \left(\sum_k \hat{a}_{q-k}\hat{m}_k\right) \mathrm{e}^{\mathrm{i}qx} + \frac{1}{N^2}\sum_q \left(\sum_k \mathrm{i}k\hat{b}_{q-k}\hat{m}_k\right) \mathrm{e}^{\mathrm{i}qx}$$

Since the exponential functions are linearly independent we can write the previous equation on vector form as

$$\dot{\hat{m}} = (\hat{F}_1 + \hat{F}_2)\cdot \hat{m}$$

Where $\hat{m}^N = (\hat{m}_1, \ldots, \hat{m}_N)^T$ and the matrices $\hat{F}_1, \hat{F}_2 \in \mathbb{C}^{N\times N}$ become

$$\hat{F}_1 = \frac{1}{N}\begin{bmatrix} \hat{a}_1 & \hat{a}_N & \cdots & \hat{a}_3 & \hat{a}_2 \\ \hat{a}_2 & \hat{a}_1 & \cdots & \hat{a}_4 & \hat{a}_3 \\ \vdots & \vdots & \ddots & \vdots & \vdots \\ \hat{a}_{N-1} & \hat{a}_{N-2} & \cdots & \hat{a}_1 & \hat{a}_N \\ \hat{a}_N & \hat{a}_{N-1} & \cdots & \hat{a}_2 & \hat{a}_1 \end{bmatrix}$$

$$\hat{F}_2 = \frac{i}{N}\begin{bmatrix} 0\hat{b}_1 & 1\hat{b}_N & \cdots & (\frac{N}{2}-1)\hat{b}_{\frac{N}{2}+2} & (-\frac{N}{2})\hat{b}_{\frac{N}{2}+1} & \cdots & -2\hat{b}_3 & -1\hat{b}_2 \\ 0\hat{b}_2 & 1\hat{b}_1 & \cdots & (\frac{N}{2}-1)\hat{b}_{\frac{N}{2}+3} & (-\frac{N}{2})\hat{b}_{\frac{N}{2}+2} & \cdots & -2\hat{b}_4 & -1\hat{b}_3 \\ \vdots & \vdots & & \vdots & \vdots & & \vdots & \vdots \\ 0\hat{b}_{N-1} & 1\hat{b}_{N-2} & \cdots & (\frac{N}{2}-1)\hat{b}_{\frac{N}{2}} & (-\frac{N}{2})\hat{b}_{\frac{N}{2}-1} & \cdots & -2\hat{b}_1 & -1\hat{b}_N \\ 0\hat{b}_N & 1\hat{b}_{N-1} & \cdots & (\frac{N}{2}-1)\hat{b}_{\frac{N}{2}+1} & (-\frac{N}{2})\hat{b}_{\frac{N}{2}} & \cdots & -2\hat{b}_2 & -1\hat{b}_1 \end{bmatrix}$$

From (2.22) we have that $\hat{a}^N = (\hat{a}_1, \ldots, \hat{a}_n)$ is a function of u_x^N while $\hat{b}^N = (\hat{b}_1, \ldots, \hat{b}_n)$ is a function of u^N. We want to write the Euler equation on the form (2.21), this means that we need to show how to calculate u^N and u_x^N as functions of $\hat{m}^N$. Inserting the fourier transform of $u^N(x)$ and $m^N(x,t)$ into $m^N = Au^N = u^N - u_{xx}^N$ yields

$$\frac{1}{N}\sum_k \hat{m}_k \mathrm{e}^{\mathrm{i}kx} = \frac{1}{N}\sum_k \hat{u}_k \mathrm{e}^{\mathrm{i}kx} + \frac{1}{N}\sum_k k^2\hat{u}_k \mathrm{e}^{\mathrm{i}kx}$$

$$\hat{m}^N = (I + D_{\mathcal{F}_N}^2)\hat{u}^N \tag{2.23}$$

Where I is the $N \times N$ identity matrix and $D_{\mathcal{F}_N} = \mathrm{diag}(-\frac{N}{2}, \ldots, \frac{N}{2}-1) \in \mathbb{R}^{N\times N}$. This linear system can be solved for $\hat{u}^N$

$$\hat{u}^N = (I + D_{\mathcal{F}_N}^2)^{-1}\hat{m}^N \tag{2.24}$$

Similarly we find

$$\hat{u}_x^N = \mathrm{i}D_{\mathcal{F}_N}\hat{u}^N = \mathrm{i}D_{\mathcal{F}_N}(I + D_{\mathcal{F}_N}^2)^{-1}\hat{m}^N$$

Algorithm 2 shows how the two matrices $\hat{F}_1$ and $\hat{F}_2$ can be computed using the above techniques, while algorithm 3 gives a summary of the final method.

(2.25)

Algorithm 2 How to calculate $\hat{F}_1$ and $\hat{F}_2$ from $\hat{m}$ using Matlab

```
N=length(mhat);
D=fftshift((-N/2:N/2-1));
uhat=(1./(1+D.^2)).*mhat;
uxhat=1i*D.*uhat;
F1=-2/N*toeplitz(uxhat,[uxhat(1);uxhat(N:-1:2)]);
F2=-1i/N*toeplitz(uhat,[uhat(1);uhat(N:-1:2)]).*repmat(D,N,1);
```

Algorithm 3 Solving the CH equation using a Lie group method

Input: initial condition u_0^N, time step size h and the output time t_{stop}.
$\hat{u}_0^N = \text{fft}(u_0^N)$.
Calculate $\hat{m}_0^N$ from $\hat{u}_0^N$ using (2.23).
for $k = 1$ to $K = \lfloor \frac{t_{stop}}{h} \rfloor$ **do**
  Calculate $\hat{m}_k^N$ with algorithm 1, using algorithm 2 to find U_r.
end for
Use (2.24) to find $\hat{u}_K^N$ from $\hat{m}_K^N$.
$u_K^N = \text{ifft}(\hat{u}_K^N)$.

There is an inefficiency in the use of the FFT in Matlab that must be mentioned. In most applications the data to be differentiated will be real, and yet, the use of the FFT makes use of a complex transform. Therefore we will sometimes experience that a real variable will become complex when differentiatied using Matlabs FFT. One can make sure that the variable m_k^N remains real by writing $\hat{m}_k^N = \text{FFT}(\text{real}(\text{iFFT}(\hat{m}_k^N)))$ after each time step. All tests will henceforth incorporate this trick as it is necessary to avoid blowup.

It is also worth investigating 2/3-rule of section 2.2. Tests indicate that the 2/3-rule will make the method more stable for large time spans, see figure 15. However, for short time spans it will decrease the accuracy, as seen in figure 14. Figure 15 shows that the Lie group integrator has advantageous long term properties compared to a finite difference scheme. Alas, the methods relies on computing several $N \times N$ matrix exponentials each time step, and is therefore considerably slower than the finite difference methods. It is also worth noting that there did not seem to be any difference in the accuracy whether one used a second or a fourth order Lie group integrator.

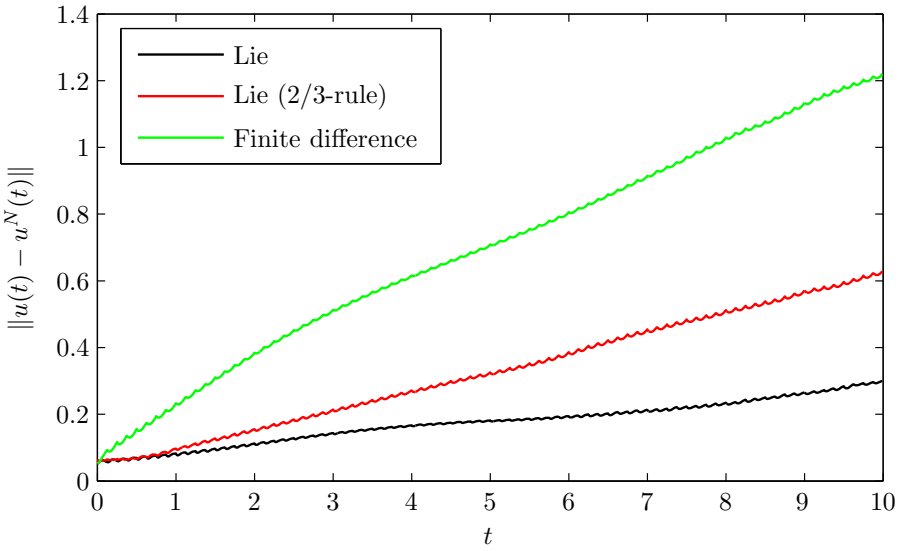

Figure 14: A comparison of the numerical error for Lie group integrators and a finite difference scheme (2.3). The Lie group integrator is more accurate, but is also considerably slower. The 2/3-rule does not appear to be advantageous here, but figure 15 shows that it does improve accuracy for larger t.

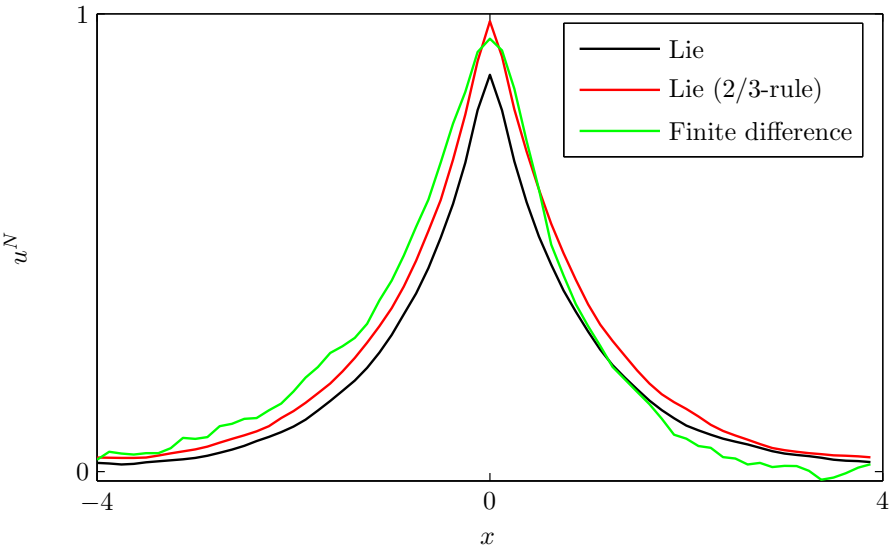

Figure 15: The approximated solution at $t = 1000$ and $N = 64$ using algorithm 3 with CFREE2, with and without the 2/3-rule. The Lie group integrator clearly preserves the peakon shape better than the finite difference scheme. However, because it needs to calculate 2 matrix exponentials per time step, it is considerably slower. In fact, the Lie group integrator used 40 minutes while the finite difference method used just 40 seconds. A smooth initial condition yields no clear difference between the three methods.

2.5 Multipeakon methods

The multipeakon methods differ from the beforementioned methods in that they assume the solution to be a linear combination of peakons. The advantage of these methods is that the numerical system to be solved usually is small. The unknowns will typically be the height, position and possibly the energy of each peakon. Compared to a finite difference scheme with $N = 512$ unknowns, these methods will certainly be faster. The disadvantage of these methods is that they only handle peakon initial conditions. The usual remedy is to approximate the nonpeakon initial condition with a linear combination of peakons such that when the number of peakons n goes to infinity the approximation converges to the initial condition. To the author's knowledge there does not exist any periodic versions of these methods yet.

There are two types of multipeakon schemes available. The first method is simply to numerically solve the system of ordinary differential equations that comes from the Hamiltonian formulation (1.6)

$$u(x,t) = \sum_{i=1}^{n} p_i(t) \mathrm{e}^{-|x-q_i(t)|} \tag{2.26}$$

where $(p_i(t), q_i(t))$ satisfy the explicit system of ordinary differential equations

$$\dot{q}_i = \sum_{j=1}^{n} p_j \mathrm{e}^{-|q_i-q_j|}, \qquad \dot{p}_i = \sum_{j=1}^{n} p_i p_j \mathrm{sgn}(q_i - q_j) \mathrm{e}^{|q_i-q_j|} \tag{2.27}$$

As before, $p_i(t)$ denotes the height and $q_i(t)$ denotes the position of peakon number i. These equations can then be solved using a suitable ODE solver, of which there are many. In the tests below we will be using Matlab's ode45.

Before we turn to the numerical tests, let us consider the other method. The method is based on changing the variables in (1.3) to Lagrangian coordinates [26], the rather comprehensive derivation can be found in [25]. The result is the following ODE

$$\left.\begin{aligned} \frac{\mathrm{d}y_i}{\mathrm{d}t} &= u_i \\ \frac{\mathrm{d}u_i}{\mathrm{d}t} &= -Q_i \\ \frac{\mathrm{d}H_i}{\mathrm{d}t} &= u_i^3 - 2P_i u_i \end{aligned}\right\} \tag{2.28}$$

Here y_i, u_i and H_i denotes the position, cumulative height and energy of each peakon. Note that y_i and q_i means the same in these two methods, while u_i and p_i do not. The distinction is that p_i means the height of each

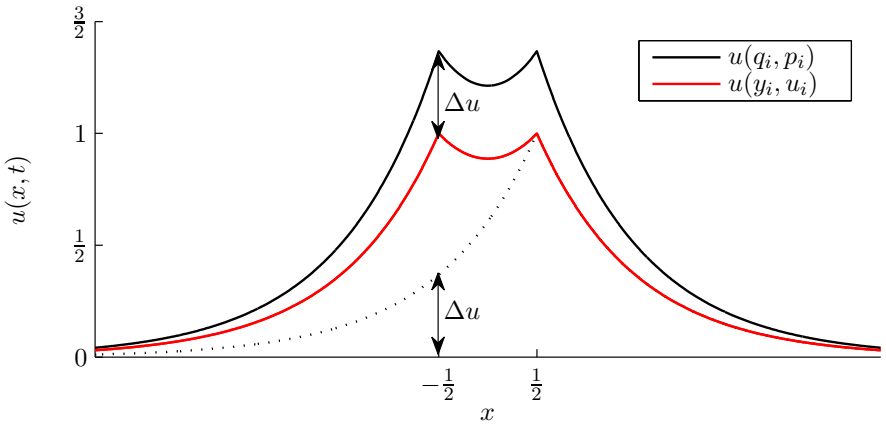

Figure 16: Two multipeakon solutions with $y = q = (-\frac{1}{2}, \frac{1}{2})^T$ and $u = p = (1,1)^T$. Note that the two multipeakons are unequal since u_i does not mean the same as p_i. Here the difference between the two at $x = -\frac{1}{2}$ is $\Delta u = \mathrm{e}^{-|-\frac{1}{2}-\frac{1}{2}|} = \mathrm{e}^{-1} \approx 0.37$.

individual peakon, while u_i also embody the height difference caused by nearby peakons. See figure 16 to better understand this distinction.

P_i and Q_i can be expressed as functions of y_i and u_i, thereby making the ODE (2.28) a well-posed $3 \times n$ dimensional system

$$P_i = \sum_{j=0}^{n} P_{ij} \qquad \text{and} \qquad Q_i = -\sum_{j=0}^{n} \kappa_{ij} P_{ij}$$

$$P_{ij} = \begin{cases} \mathrm{e}^{(y_1 - y_i)} \frac{u_1^2}{4} & \text{for } j = 0 \\ \dfrac{\mathrm{e}^{\kappa_{ij} y_i} \mathrm{e}^{\kappa_{ij} \bar{y}_j}}{8 \cosh(\delta y_j)} [2\delta H_j \cosh^2(\delta y_j) & \\ \quad + 8\kappa_{ij} \bar{u}_j \delta u_j \sinh^2(\delta y_j) + 4\bar{u}_j^2 \tanh(\delta y_j) & \text{for } j = 1, \ldots, n-1 \\ \mathrm{e}^{(y_i - y_n)} \frac{u_n^2}{4} & \text{for } j = n \end{cases}$$

Where the following variables are introduced to simplify the notation

$$\bar{y}_i = \frac{1}{2}(y_{i+1} + y_i) \quad \text{and} \quad \delta y_i = \frac{1}{2}(y_{i+1} - y_i);$$

$$\kappa_{ij} = \begin{cases} -1 & \text{if } j \geq i \\ 1 & \text{otherwise} \end{cases}$$

Using (2.26) one can calculate $u(x,t)$ from (p_i, q_i). Since q_i and u_i do not mean the same, one can not use this equation to find $u(x,t)$ from (y_i, u_i). We know that between two adjacent peaks located at y_i and y_{i+1}, u satisfies $u - u_{xx} = 0$ and therefore u can be written as

$$u(x) = A_i \mathrm{e}^x + B_i \mathrm{e}^x \text{ for } x \in [y_i, y_{i+1}], \quad i = 1, \ldots, n-1 \tag{2.29}$$

where the constants A_i og B_i depend on u_i, u_{i+1}, y_i and y_{i+1}.

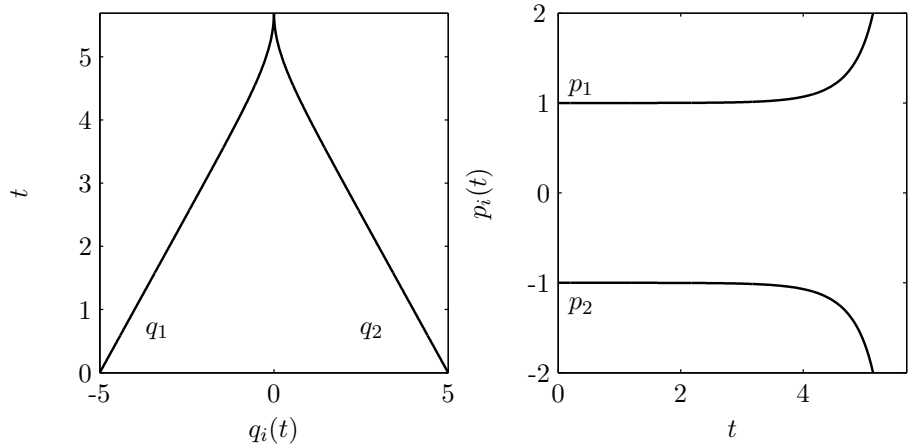

Figure 17: Peakon-antipeakon collision approximated with the first multipeakon method (2.27). The result is the dissipative solution. Notice that the solution vanishes since $p_1 = -p_2$ and $q_1 \to q_2$.

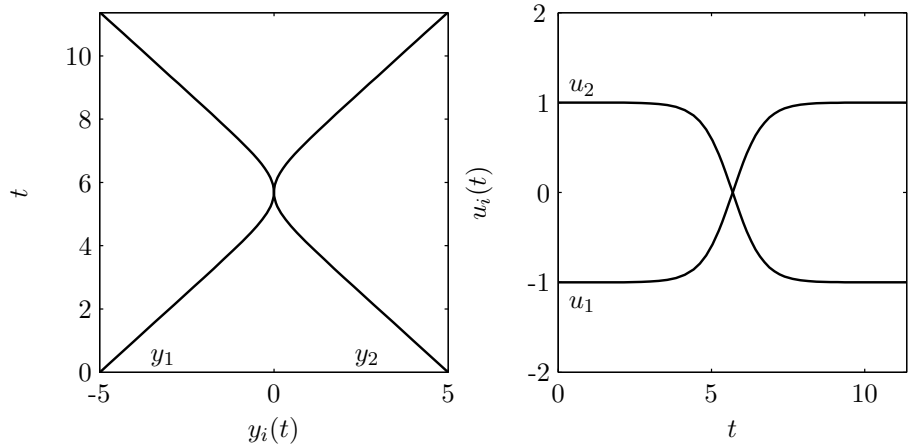

Figure 18: Peakon-antipeakon collision approximated with the second multipeakon method (2.28). This method produces the conservative solution where the peakons re-emerge after the collision.

3 Comparison of the numerical methods

In the previous chapter we have studied the strengths and weaknesses of the numerical methods. Now, we wish to do an objective comparison of the seven methods presented below.

- **FD1**: The one-sided finite difference scheme (2.4).
- **FD1m**: The modified finite difference scheme (2.3) using central differences.
- **FD2**: The finite difference scheme (2.8).
- **Sp**: The spectral method (2.9).
- **Sp23**: The spectral method (2.10) using the 2/3-rule.
- **MS**: The Euler box scheme applied to a 8×8 multisymplectic formulation [14].
- **Lie**: Algorithm 3 using the Lie group integrator CFREE2.

Since the multipeakon methods of section 2.5 are not periodic, they will not be compared to the other methods here.

There are three different qualities we have considered: the global error, conservation of the Hamiltonians found in section 1.2 and the running time. To avoid long-lasting running times and to save space the spatial resolution is set relatively low at $N = 64$. Tests show that the relations between the methods stays the same for higher N. The conservation properties of the different Hamiltonians $\mathscr{H}_i$ is similar, and we will therefore only consider $\mathscr{H}_1$ (1.20). We will, however, need to distinguish between smooth and non-smooth initial conditions. The smooth initial condition will be the left one in figure 5 and the non-smooth a periodic peakon initial condition (1.5) on the interval $[-4, 4]$.

The figures 19 and 20 show $\mathscr{H}_1$ with a smooth and non-smooth initial condition respectively. The finite difference schemes **FD1** and **FD2** suffer from damping which ruins the conservation properties. The rest of the methods perform similarly on the smooth initial condition, however the spectral methods **Sp** and **Sp23** are marginally better. In figure 20 we see that both **Sp** and **MS** blow up when the initial condition is non-smooth. We also know from chapter 2.2 that **Sp23** is prone to blow up.

Figure 21 shows the global error after one period on the interval $[-4, 4]$. The figure looks similar for the smooth initial condition. The spectral and multisymplectic methods perform well when the time span is short. The finite difference methods are very stable, however they are not the most accurate in this experiment.

Note that the Lie group method is one of the best methods in the figures 19, 20 and 21, and we know it is stable in the long run. However figure 22 shows that it is considerably slower than the other methods. By finding a way to avoid computing large matrix exponentials each time step, the Lie group method could be a viable method for solving the Euler equation and thus the Camassa-Holm equation.

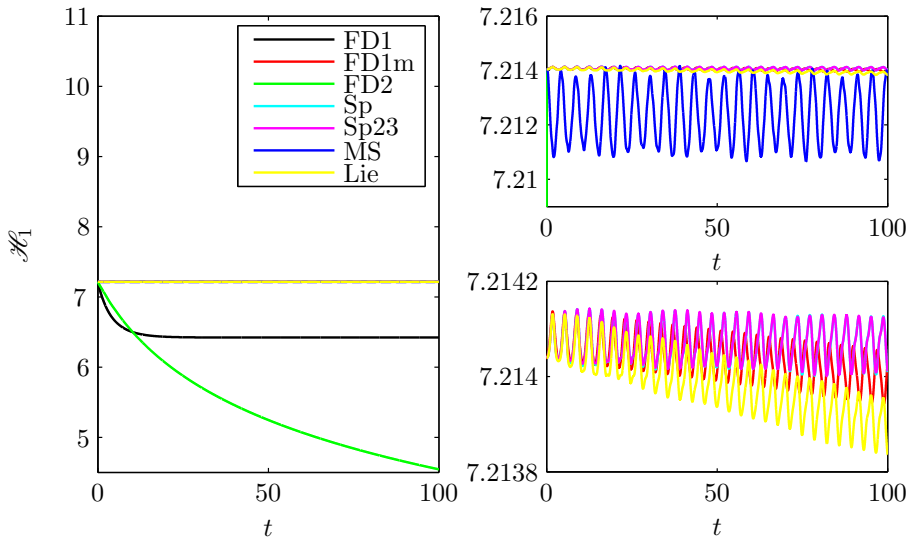

Figure 19: This is a plot of the conserved quantity $\mathscr{H}_1$ approximated with $N = 64$ and a smooth initial condition. The plots on the right are magnified versions of the one on the left.

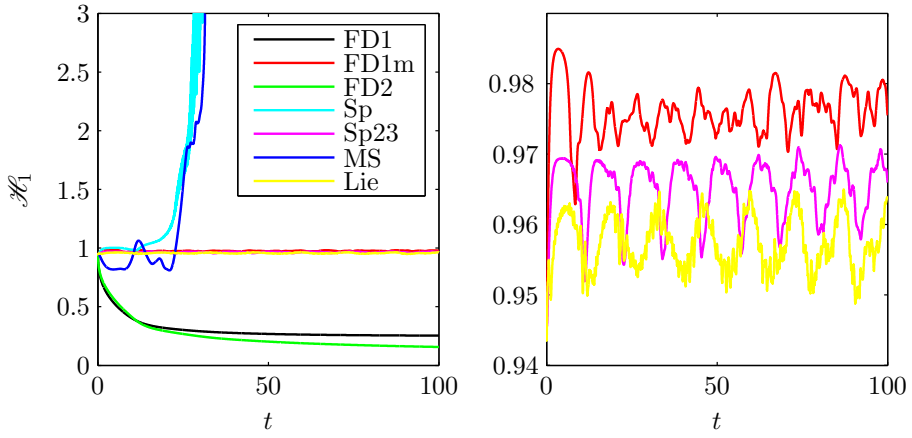

Figure 20: $\mathscr{H}_1$ approximated with $N = 64$ and a peakon initial condition. The plot on the right is a magnificaiton of the one on the left.

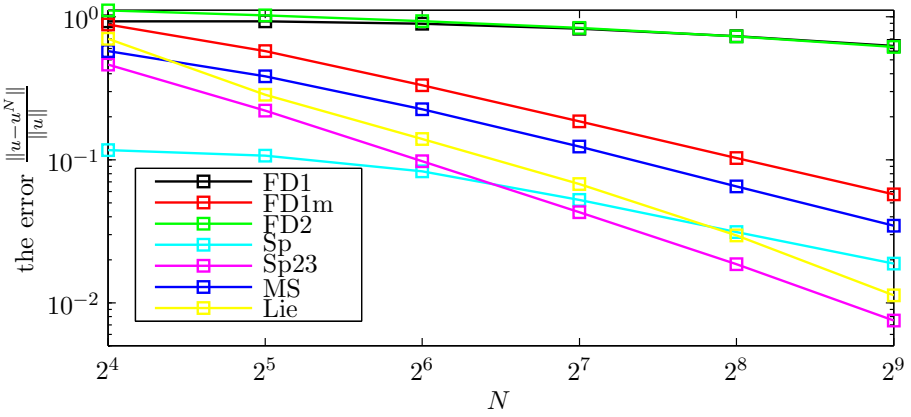

Figure 21: The global numerical error with respect to the spatial resolution N for different numerical methods. The initial condition is a single peakon on the interval $[-4, 4]$ and the error is calculated after one period.

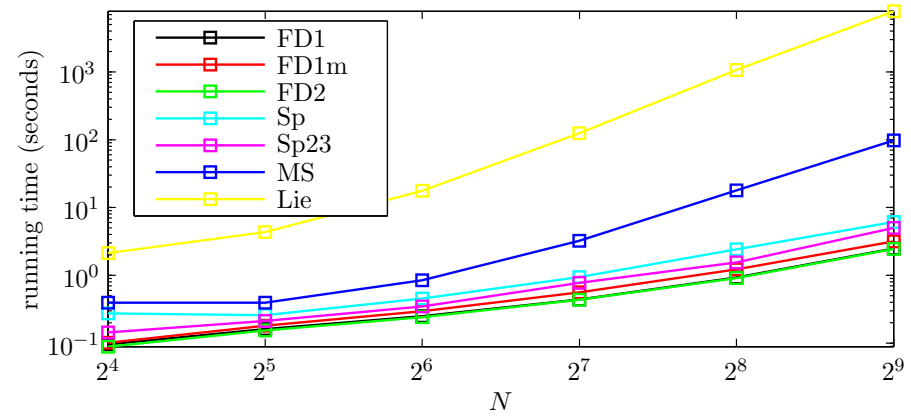

Figure 22: This is a plot of the running time for the calculations done in figure 21.

4 Conclusion

We have shown that the Camassa-Holm equation is the Euler equation describing the geodesic flow on the Lie group of diffeomorphisms on the circle with respect to the right-invariant H^1-metric. This was done using the geometrical approach initiated by Arnold and Khesin [3]. By choosing other groups and metrics one can arrive at many well-known equations in mathematical physics such as the Burgers equation, the Korteweg-de Vries equation and the Hunter-Saxton equation. By following the methodology of Olver [40] we showed that the Camassa-Holm equation can be expressed as a bi-Hamiltonian system, and that this leads to infinitely many conserved quantities.

By freezing coefficients in the Euler equation and applying a Lie group integrator we derived a numerical procedure of solving the Camassa-Holm equation. The method performed better than existing methods in some situations, as it stands, however, the method is not ready to replace other numerical solvers as the numerical cost is still too high. Nevertheless, since the method can be used to solve the class of equations following from the Euler equation, the method is an interesting direction in geometric integration.

We reviewed the existing numerical methods of solving the Camssa-Holm equation and tested them on smooth and non-smooth periodic initial conditions. The methods behaved similarly when the initial condition was smooth, but in the non-smooth peakon case we saw some differences. We studied the long term behaviour of the error and the conservation of the Hamiltonians. The finite difference method using central differences performed considerably better than the one-sided schemes which suffered from damping. The spectral methods and the multisymplectic method was accurate for short time spans, but the solution blew up in long time approximations for non-smooth initial conditions. The multipeakon methods were superior to the other methods, however these are not yet extended to the periodic case. Apart from the multipeakon methods, the multisymplectic method was the only method that produced the conservative solution in the peakon-antipeakon case, however also the multisymplectic method showed instabilities.

The frozen coefficients method showed good structure preserving properties, but was considerably slower then the other methods since the Lie group methods need to calculate several matrix exponentials in each time step. However, the Lie group method can be replaced by, for instance, a particle method solving the equation in characteristic variables. This could be the topic of future research.

References

[1] V. I. Arnold. *Mathematical methods of classical mechanics*, volume 60 of *Graduate Texts in Mathematics*. Springer-Verlag, New York. Translated from the 1974 Russian original by K. Vogtmann and A. Weinstein, Corrected reprint of the second (1989) edition.

[2] V. I. Arnold. Sur la géométrie différentielle des groupes de Lie de dimension infinie et ses applications à l'hydrodynamique des fluides parfaits. *Ann. Inst. Fourier (Grenoble)*, 16(fasc. 1):319–361, 1966.

[3] V. I. Arnold and B. A. Khesin. *Topological methods in hydrodynamics*, volume 125 of *Applied Mathematical Sciences*. Springer-Verlag, New York, 1998.

[4] R. Artebrant and H. J. Schroll. Numerical simulation of Camassa-Holm peakons by adaptive upwinding. *Appl. Numer. Math.*, 56(5):695–711, 2006.

[5] R. Beals, D. H. Sattinger, and J. Szmigielski. Multi-peakons and a theorem of stieltjes. *Inverse Problems*, 15(1):L1–L4, 1999.

[6] R. Beals, D. H. Sattinger, and J. Szmigielski. Multipeakons and the classical moment problem. *Adv. Math.*, 154(2):229–257, 2000.

[7] T. J. Bridges. Multi-symplectic structures and wave propagation. *Math. Proc. Cambridge Philos. Soc.*, 121(1):147–190, 1997.

[8] T. J. Bridges and S. Reich. Multi-symplectic integrators: numerical schemes for Hamiltonian PDEs that conserve symplecticity. *Phys. Lett. A*, 284(4-5):184–193, 2001.

[9] R. Camassa and D. D. Holm. An integrable shallow water equation with peaked solitons. *Phys. Rev. Lett.*, 71(11):1661–1664, Sep 1993.

[10] R. Camassa, D. D. Holm, and J. Hyman. A new integrable shallow water equation. *Adv. Appl. Mech.*, 31:1–33, 1994.

[11] C. Canuto, M. Y. Hussaini, A. Quarteroni, and T. A. Zang. *Spectral methods in fluid dynamics*. Springer Series in Computational Physics. Springer-Verlag, New York, 1988.

[12] E. Celledoni, A. Marthinsen, and B. Owren. Commutator-free lie group methods. *Future Generation Computer Systems*, 19(3):341–352, 2003.

[13] G.M Coclite, K.H Karlsen, and N.H. Risebro. A convergent finite difference scheme for the camassa-holm equation with general h1 initial data. 2006.

[14] D. Cohen, B. Owren, and X. Raynaud. Multisymplecticity and the camassa-holm equation (not yet published). 2007.

[15] A. Constantin and J. Escher. Global existence and blow-up for a shallow water equation. *Ann. Scuola Norm. Sup. Pisa Cl. Sci. (4)*, 26(2):303–328, 1998.

[16] A. Constantin and J. Escher. Wave breaking for nonlinear nonlocal shallow water equations. *Acta Math.*, 181(2):229–243, 1998.

[17] A. Constantin and B. Kolev. On the geometric approach to the motion of inertial mechanical systems. *J. Phys. A*, 35(32):R51–R79, 2002.

[18] A. Constantin and B. Kolev. Geodesic flow on the diffeomorphism group of the circle. *Comment. Math. Helv.*, 78(4):787–804, 2003.

[19] A. Constantin and L. Molinet. Global weak solutions for a shallow water equation. *Comm. Math. Phys.*, 211(1):45–61, 2000.

[20] L. Euler. *Leonhardi Euleri theoria motus corporum solidorum seu rigidorum ex primis nostrae cognitionis principiis stabilita et ad onmes motus qui in huiusmodi corpora cadere possunt accommodata. Vol. prius.* Edited by Charles Blanc. Leonhardi Euleri Opera Omnia (Series secunda. Opera mechanica et astronomica, Vol. III). Natural Science Society of Switzer land. Orell Füssli, Zürich, 1948.

[21] B. Fuchssteiner and A. S. Fokas. Symplectic structures, their bäcklund transformations and hereditary symmetries. *Phys. D*, 4(1):47–66, 1981/82.

[22] R. Guillermo. On the Cauchy problem for the Camassa-Holm equation. *Nonlinear Anal.*, 46(3, Ser. A: Theory Methods):309–327, 2001.

[23] H. Holden and X. Raynaud. Convergence of a finite difference scheme for the Camassa-Holm equation. *SIAM J. Numer. Anal.*, 44(4):1655–1680 (electronic), 2006.

[24] H. Holden and X. Raynaud. A convergent numerical scheme for the camassa-holm equation based on multipeakons. *Discrete Contin. Dyn. Syst*, 14(3):505–523, 2006.

[25] H. Holden and X. Raynaud. Global conservative multipeakon solutions of the Camassa-Holm equation. *To appear in the proceedings of the 11th International Conference on Hyperbolic Problems.*, 2006.

[26] H. Holden and X. Raynaud. Global conservative solutions of the Camassa-Holm equation – a lagrangian point of view. *To appear in Communications on Partial Differential Equations.*, 2006.

[27] A. Iserles, H. Z. Munthe-Kaas, S. P. Nørsett, and A. Zanna. Lie-group methods. In *Acta numerica, 2000*, volume 9 of *Acta Numer.*, pages 215–365. Cambridge Univ. Press, Cambridge, 2000.

[28] H. Kalisch. Stability of solitary waves for a nonlinearly dispersive equation. *Discrete Contin. Dyn. Syst.*, 10(3):709–717, 2004.

[29] H. Kalisch and J. Lenells. Numerical study of traveling-wave solutions for the Camassa-Holm equation. *Chaos Solitons Fractals*, 25(2):287–298, 2005.

[30] H. Kalisch and X. Raynaud. Convergence of a spectral projection of the Camassa-Holm equation. *Numer. Methods Partial Differential Equations*, 22(5):1197–1215, 2006.

[31] B. Khesin. Topological fluid dynamics. *Notices Amer. Math. Soc.*, 52(1):9–19, 2005.

[32] B. Khesin and G. Misiołek. Euler equations on homogeneous spaces and Virasoro orbits. *Adv. Math.*, 176(1):116–144, 2003.

[33] P. Kim and P. J. Olver. Geometric integration via multi-space. *Regul. Chaotic Dyn.*, 9(3):213–226, 2004.

[34] J. Lenells. Conservation laws of the Camassa-Holm equation. *J. Phys. A*, 38(4):869–880, 2005.

[35] Y. A. Li and P. J. Olver. Well-posedness and blow-up solutions for an integrable nonlinearly dispersive model wave equation. *J. Differential Equations*, 162(1):27–63, 2000.

[36] J. E. Marsden, S. Pekarsky, S. Shkoller, and Matthew West. Variational methods, multisymplectic geometry and continuum mechanics. *J. Geom. Phys.*, 38(3-4):253–284, 2001.

[37] J. E. Marsden and T. S. Ratiu. *Introduction to mechanics and symmetry*, volume 17 of *Texts in Applied Mathematics*. Springer-Verlag, New York, second edition, 1999. A basic exposition of classical mechanical systems.

[38] J. E. Marsden and S. Shkoller. Multisymplectic geometry, covariant Hamiltonians, and water waves. *Math. Proc. Cambridge Philos. Soc.*, 125(3):553–575, 1999.

[39] B. Moore and S. Reich. Backward error analysis for multi-symplectic integration methods. *Numer. Math.*, 95(4):625–652, 2003.

[40] P. J. Olver. *Applications of Lie groups to differential equations*, volume 107 of *Graduate Texts in Mathematics*. Springer-Verlag, New York, second edition, 1993.

[41] S. Reich. Multi-symplectic Runge-Kutta collocation methods for Hamiltonian wave equations. *J. Comput. Phys.*, 157(2):473–499, 2000.

[42] V. S. Varadarajan. *Lie groups, Lie algebras, and their representations*, volume 102 of *Graduate Texts in Mathematics*. Springer-Verlag, New York, 1984. Reprint of the 1974 edition.

[43] Z. Xin and P. Zhang. On the weak solutions to a shallow water equation. *Comm. Pure Appl. Math.*, 53(11):1411–1433, 2000.

[44] Y. Xu and C. Shu. A local discontinuous galerkin method for the camassa-holm equation. 2007.